FLORE
Repository istituzionale dell'Università degli Studi di Firenze

(+)-Catharanthine potentiates the GABAA receptor by binding to a transmembrane site at the β(+)/α(-) interface near the TM2-TM3 loop

Questa è la Versione finale referata (Post print/Accepted manuscript) della seguente pubblicazione:

Original Citation:

(+)-Catharanthine potentiates the GABAA receptor by binding to a transmembrane site at the β(+)/α(-) interface near the TM2-TM3 loop / Arias, Hugo R; Borghese, Cecilia M; Germann, Allison L; Pierce, Spencer R; Bonardi, Alessandro; Nocentini, Alessio; Gratteri, Paola; Thodati, Thanvi M; Lim, Natalie J; Harris, R Adron; Akk, Gustav. - In: BIOCHEMICAL PHARMACOLOGY. - ISSN 1873-2968. - ELETTRONICO. - 199:(2022), pp. 114993-114993. [10.1016/j.bcp.2022.114993]

Availability:

This version is available at: 2158/1289762 since: 2022-11-14T07:09:15Z

Published version:

DOI: 10.1016/j.bcp.2022.114993

Terms of use:

Open Access

La pubblicazione è resa disponibile sotto le norme e i termini della licenza di deposito, secondo quanto stabilito dalla Policy per l'accesso aperto dell'Università degli Studi di Firenze (https://www.sba.unifi.it/upload/policy-oa-2016-1.pdf)

Publisher copyright claim:

Conformità alle politiche dell'editore / Compliance to publisher's policies

Questa versione della pubblicazione è conforme a quanto richiesto dalle politiche dell'editore in materia di copyright.

This version of the publication conforms to the publisher's copyright policies.

(Article begins on next page)

30 June 2024

Author Manuscript

Author Manuscript

Author Manuscript

Author Manuscript

HHS Public Access

Author manuscript

Biochem Pharmacol. Author manuscript; available in PMC 2023 May 01.

Published in final edited form as:

Biochem Pharmacol. 2022 May ; 199: 114993. doi:10.1016/j.bcp.2022.114993.

(+)-Catharanthine potentiates the $GABA_A$ receptor by binding to a transmembrane site at the β(+)/α(−) interface near the TM2-TM3 loop

Hugo R. Arias[*,a,1], **Cecilia M. Borghese**[b,1], **Allison L. Germann**[c], **Spencer R. Pierce**[c], **Alessandro Bonardi**[e], **Alessio Nocentini**[e], **Paola Gratteri**[*,e], **Thanvi M. Thodati**[b], **Natalie J. Lim**[b], **R. Adron Harris**[b], **Gustav Akk**[c,d]

[a]Department of Pharmacology and Physiology, Oklahoma State University College of Osteopathic Medicine, Tahlequah, OK, USA.

[b]Waggoner Center for Alcohol and Addiction Research, The University of Texas at Austin, Austin, TX, USA.

[c]Department of Anesthesiology, Washington University School of Medicine, St. Louis, MO, USA.

[d]Taylor Family Institute for Innovative Psychiatric Research, Washington University School of Medicine, St. Louis, MO, USA.

[e]Department of Neurosciences, Psychology, Drug Research and Child Health (NEUROFARBA), Section of Pharmaceutical and Nutraceutical Sciences, Laboratory of Molecular Modeling Cheminformatics & QSAR, University of Florence, Florence, Italy.

Abstract

(+)-Catharanthine, a coronaridine congener, potentiates the γ-aminobutyric acid type A receptor ($GABA_AR$) and induces sedation through a non-benzodiazepine mechanism, but the specific site of action and intrinsic mechanism have not been defined. Here, we describe $GABA_AR$ subtype selectivity and location of the putative binding site for (+)-catharanthine using electrophysiological, site-directed mutagenesis, functional competition, and molecular docking

[*]Corresponding author pre-publication: Dr. Cecilia M. Borghese, Waggoner Center for Alcohol and Addiction Research, The University of Texas at Austin, Austin, TX, USA; cborghese@austin.utexas.edu. Corresponding authors post-publication: Dr. Hugo R. Arias, Department of Pharmacology and Physiology, Oklahoma State University College of Osteopathic Medicine, Tahlequah, OK 74464, USA; hugo.arias@okstate.edu; Tel: +1 (918) 525-6324. Prof. Paola Gratteri, paola.gratteri@unifi.it.

[1]These authors contributed equally to this work.

Publisher's Disclaimer: This is a PDF file of an unedited manuscript that has been accepted for publication. As a service to our customers we are providing this early version of the manuscript. The manuscript will undergo copyediting, typesetting, and review of the resulting proof before it is published in its final form. Please note that during the production process errors may be discovered which could affect the content, and all legal disclaimers that apply to the journal pertain.

Declarations of interest: none

Credit Author Statement

Hugo Arias: Conceptualization, Formal analysis, Writing – Original draft and Review and Editing, Visualization, Project administration, Supervision, Resources. **Cecilia Borghese**: Formal analysis, Investigation, Writing – Original draft and Review and Editing, Visualization, Project administration. **Allison Germann:** Investigation, Formal analysis**. Spencer Pierce**: Investigation, Formal analysis. **Alessandro Bonardi**: Investigation, Formal analysis. **Alessio Nocentini**: Investigation, Formal analysis. **Paola Gratteri**: Investigation, Formal analysis, Writing – Original draft and Review and Editing, Visualization. **Thanvi Thodati**: Investigation, Formal analysis. **Natalie Lim**: Investigation, Formal analysis. **Adron Harris**: Resources, Writing – Review & Editing, Funding acquisition. **Gustav Akk**: Resources, Conceptualization, Formal analysis, Writing - Review and Editing, Funding acquisition, Supervision

Author Manuscript Author Manuscript Author Manuscript Author Manuscript

experiments. Electrophysiological and *in silico* experiments showed that (+)-catharanthine potentiates the responses to low, subsaturating GABA at β2/3-containing $GABA_A$Rs 2.4–3.5 times more efficaciously than at β1-containing $GABA_A$Rs. The activity of (+)-catharanthine is reduced by the β2(N265S) mutation that decreases $GABA_A$R potentiation by loreclezole, but not by the β3(M286C) or α1(Q241L) mutations that reduce receptor potentiation by R(+)-etomidate or neurosteroids, respectively. Competitive functional experiments indicated that the binding site for (+)-catharanthine overlaps that for loreclezole, but not those for R(+)-etomidate or potentiating neurosteroids. Molecular docking experiments suggested that (+)-catharanthine binds at the β(+)/α(−) intersubunit interface near the TM2-TM3 loop, where it forms H-bonds with β2-D282 (TM3), β2-K279 (TM2-TM3 loop), and β2-N265 and β2-R269 (TM2). Site-directed mutagenesis experiments supported the *in silico* results, demonstrating that the K279A and D282A substitutions, that lead to a loss of H-bonding ability of the mutated residue, and the N265S mutation, impair the gating efficacy of (+)-catharanthine. We infer that (+)-catharanthine potentiates the $GABA_A$R through several H-bond interactions with a binding site located in the β(+)/α(−) interface in the transmembrane domain, near the TM2-TM3 loop, where it overlaps with loreclezole binding site.

Graphical Abstract

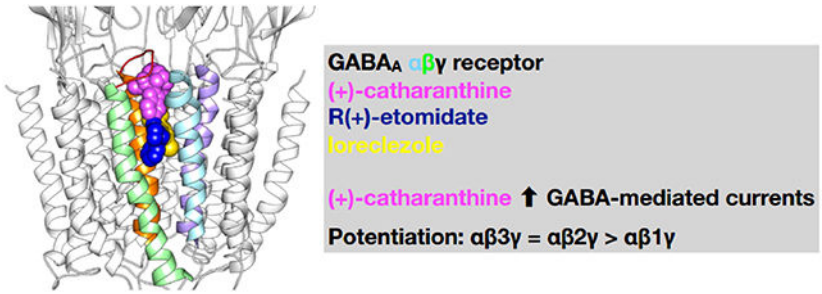

Keywords

(+)-catharanthine; Coronaridine congeners; Positive allosteric modulators; Electrophysiology; Molecular docking; Molecular dynamics

1. Introduction

Coronaridine congeners, including plant alkaloids [e.g., (−)-ibogaine and its metabolite noribogaine, (−)-coronaridine, and (+)-catharanthine] and the synthetic derivative 18-methoxycoronaridine (18-MC), decrease self-administration of drugs of abuse such as cocaine, ethanol, morphine, methamphetamine, and nicotine in animal models, and reduce drug craving and relapse in humans, making them significant lead compounds for anti-addictive therapies [1, 2]. The current notion is that their anti-addictive activity is mediated by selective inhibition of α3β4-containing nicotinic acetylcholine receptors (AChRs) expressed in the habenula [1, 3]. Based on encouraging preclinical studies, several of these congeners are in clinical trials for opioid use disorder, including noribogaine [Phase 1; [4]], 18-MC (Phase 1), and ibogaine (Phase 1/2a). Given the beneficial effects of (−)-ibogaine

Author Manuscript Author Manuscript Author Manuscript Author Manuscript

for treatment of opioid use disorder [5], this drug is currently utilized clinically in several countries, including the U.S.

Animal studies have shown that coronaridine congeners have, in addition to anti-addictive activity, antidepressant, anxiolytic, anti-obesity, and anti-neuropathic activity [1, 6, 7]. We previously reported sedative activity of (+)-catharanthine (Fig. 1) that is likely mediated by potentiation of γ-aminobutyric acid type A receptors ($GABA_ARs$) [8]. Although most of the studies to determine the mechanisms underlying the anti-addictive and anti-nociceptive effects of coronaridine congeners have been oriented toward AChRs, it is plausible that modulation of $GABA_ARs$ also plays a role in these activities, considering that these receptors are involved in pain [9] and addiction [10]. In this regard, determining the functional and structural features of the interaction of (+)-catharanthine with the $GABA_AR$ is an important and necessary step for the advancement of this hypothesis and might help to shed light on the anti-addictive properties of these compounds given that several other $GABA_AR$ potentiators, including benzodiazepines, barbiturates, and ethanol, can induce tolerance and dependence [11–14]. Thus, the information obtained in this work will be helpful in the development of derivatives for different pharmacotherapeutic purposes.

Here, we have characterized the putative binding site and molecular mechanisms underlying the potentiating activity of (+)-catharanthine on $GABA_ARs$, using a combination of functional and structural approaches. Using electrophysiology, we assessed $GABA_AR$ subtype specificity and examined the effects of mutations to known binding sites of several positive allosteric modulators of the $GABA_AR$ on modulation by (+)-catharanthine. Functional competition assay was employed to determine structural overlap between the sites mediating the effects of (+)-catharanthine and loreclezole, R(+)-etomidate or potentiating neurosteroids. To support functional data, molecular docking and molecular dynamics (MD) experiments were performed using a series of homology-built models of the wild-type and mutant $GABA_AR$ employing as template the cryo-electron microscopy structure of the human α1β3γ2L $GABA_AR$ (PDB: 6HUJ) [15].

2. Materials and Methods

2.1. Materials

R(+)-Etomidate was purchased from Tocris (Bio-Techne Corp., Minneapolis, MN, USA) or Toronto Research Chemicals Inc (North York, Ontario, Canada). GABA, propofol, loreclezole, and picrotoxin were purchased from Sigma-Aldrich (St. Louis, MO, USA). (+)-Catharanthine (free base) was obtained from Henan Tianfu Chemical Co. (Zhengzhou, China). (+)-Catharanthine hydrochloride, a gift from Dr. Kuehne (University of Vermont, VT, USA), was synthesized as described previously [16]. Salts, solvents, and reagents were purchased from *Sigma-Aldrich (St. Louis, MO)*.

Stock solutions of (+)-catharanthine hydrochloride and free base (100–300 mM), loreclezole (10 mM), propofol (200 mM), and R(+)-etomidate (200 mM) were prepared in DMSO and subsequently diluted with bath solution on the day of experiment. The solubility of each drug in the solutions was assessed by visual inspection. No precipitation was observed at the highest concentration used. The maximal concentration of DMSO in working solutions

Author Manuscript Author Manuscript Author Manuscript Author Manuscript

was 0.3%. We have previously shown that DMSO at up to 0.5% is without effect on holding current or GABA-elicited responses [17].

2.2. Constructs and expression

The complementary DNAs encoding rat $GABA_A$ α1, β1, β2, β3, γ2S and γ2L (provided by Dr. M.H. Akabas), and human α2 (provided by Dr. N.L. Harrison) and β2 subunits (provided by Dr. P.J. Whiting) were subcloned into pGEMHE or pcDNA3 expression vectors. Mutations in the α and β subunits were made using QuikChange (Agilent Technologies, CA, USA) or purchased from Twist Bioscience (South San Francisco, CA, USA). The *in vitro* transcription of $GABA_A$ subunits was performed using mMessage mMachine (Life Technologies, Grand Island, NY, USA). The cRNAs were recovered using phenol:chloroform extraction and isopropanol precipitation. After resuspension in nuclease-free water, the cRNAs were quantified using NanoDrop 2000 (Thermo Fisher Scientific, Waltham, MA, USA) or Bioanalyzer (Agilent, Santa Clara, CA, USA) spectrophotometers.

Oocytes were harvested from African clawed frog (*Xenopus laevis*), purchased from Nasco (Fort Atkinson, WI, USA), and treated according with the ARRIVE guidelines. The frogs were anesthetized with tricaine and a partial ovariectomy performed following a protocol approved by The University of Texas at Austin IACUC and in accordance with the National Institutes of Health Guide for the Care and Use of Laboratory Animals. These oocytes, or oocytes purchased from Xenopus1 (Dexter, MI, USA), were injected with 3.5–6.0 ng of capped complementary RNAs (in the volume of 50 nL) per oocyte in 1:1:10 (αβ1γ2), 1:1:5 or 1:1:10 (αβ2γ2), or 1:0.6:10 (αβ3γ2) ratios. The injected oocytes were incubated at 15 °C in sterilized Modified Barth's solution (88 mM NaCl, 1 mM KCl, 2.4 mM $NaHCO_3$, 10 mM HEPES, 0.82 mM $MgSO_4$, 0.33 mM $Ca(NO_3)_2$, 0.91 mM $CaCl_2$, supplemented with 10,000 U/L penicillin, 10 mg/L streptomycin, 50 mg/L gentamycin, 90 mg/L theophylline and 220 mg/L pyruvate, pH = 7.5) for 2–5 days before recording.

2.3. Electrophysiological recordings of wild-type and mutant $GABA_AR$ subtypes expressed in *Xenopus laevis* oocytes

The electrophysiological experiments were conducted using the standard two-electrode voltage clamp technique. The oocytes were placed in an RC-1Z recording chamber (Warner Instruments, Hamden, CT, USA) or a custom-made acrylic recording chamber (100 μl volume), and clamped at −70 to −60 mV. The voltage and current electrodes were borosilicate glass capillaries (G120F-4, OD = 1.20 mm, ID = 0.69 mm; Warner Instruments, or 30-31-0-075, OD = 1.20 mm, ID = 0.9 mm; FHC, Bowdoin, ME, USA). The electrodes were filled with 3 M KCl. The bath solution (ND96) contained 96 mM NaCl, 2 mM KCl, 1.8 mM $CaCl_2$, 1 mM $MgCl_2$, 5 mM HEPES (pH 7.4). All experiments were conducted at room temperature.

The current responses were amplified with an OC-725C (Warner Instruments) or Axoclamp 900A amplifier (Molecular Devices, San Jose, CA, USA), digitized with a Digidata 1200 or 1320 series (Molecular Devices) or PowerLab 4/30 (ADInstruments Inc, Colorado Springs, CO, USA) digitizer, and stored on a PC hard drive. Analysis of current traces was done using Clampfit (Molecular Devices).

Author Manuscript Author Manuscript Author Manuscript Author Manuscript

To verify the presence of the γ2 subunit in the expressed receptors, 10 μM $ZnCl_2$ was pre-applied alone for 60 s followed by its co-application with GABA. Oocytes tested with $ZnCl_2$ showed small inhibition of GABA responses [−14 ± 4% for α1βxγ2, −26 ± 6% for α1β3(M286C)γ2S] or even potentiation [+11 ± 1% for α1β2(N265S)γ2S], indicating the expression of ternary $GABA_A$Rs, as αβ receptors show near 100% inhibition at this Zn^{2+} concentration [18].

The effects of (+)-catharanthine among different $GABA_A$R subtypes were studied at a concentration of GABA that induces 5% activation (EC_5). To identify the EC_5 GABA concentration, a saturating (1 mM) concentration of GABA was applied for 20 s, and after a 15 min washout, several GABA concentrations in the low μM range were tested until identifying one that produced 3–7% of the maximal response (nominal EC_5). We then proceeded to use that GABA concentration to study the effects of (+)-catharanthine in the same oocyte. After two consecutive applications of EC_5 GABA, (+)-catharanthine was co-applied with EC_5 GABA, followed by another application of EC_5 GABA to demonstrate washout of the effect. The experiments on receptors containing the α1(Q241L), β3(M286C), or β2(N265S) mutated subunits were performed following similar protocols, activating the receptors with a low ($EC_{5–15}$) concentration of GABA. The potentiating effect of a modulator was calculated as ($I_{peak,GABA+modulator}$ / $I_{peak,GABA}$) - 1, and expressed as % change in response to GABA.

The degree of potentiation by positive allosteric modulators (PAMs) depends on the level of activity of the control response to low GABA; larger potentiating effects are observed at lower levels of control activity. In these experiments, the level of activity in the presence of low GABA was indistinguishable within each wild-type and mutant pair ($P > 0.05$; data not shown).

2.4. Mechanistic analysis of $GABA_A$R activation or potentiation by (+)-catharanthine, loreclezole, and R(+)-etomidate

The concentration-response relationships for receptor potentiation by (+)-catharanthine or loreclezole were measured by exposing oocytes to a low concentration of GABA in the absence and presence of 0.3–100 μM (+)-catharanthine or 0.03–30 μM loreclezole. The concentrations of GABA (0.2–10 μM) in these experiments were selected to generate a response with a peak probability of being in the active state (P_A) of 0.15–0.25 (approximately $EC_{17–28}$). We note that this level of background activity is higher than that in experiments aimed at elucidating receptor subtype-selectivity (EC_5). This was done to ensure saturation of concentration-response relationships, in accordance with a prior finding that the EC_{50} of a potentiator is reduced as the P_A of background activity is increased [19]. The β2(K279A) mutant exhibited a large degree of constitutive activity ($P_{A,constitutive}$ = 0.22); accordingly, the (+)-catharanthine concentration-response relationship in this mutant was measured in the absence of GABA. The concentration-response relationship for R(+)-etomidate was measured by exposing oocytes to 1–300 μM R(+)-etomidate in the absence of other agonists, including GABA. Each oocyte was exposed to the full range of drug concentrations.

Author Manuscript Author Manuscript Author Manuscript Author Manuscript

To estimate the P_A of a current response, its peak amplitude was normalized to the peak response to 1 mM GABA + 50 μM propofol tested in the same oocyte (see Fig. 3A). The latter was considered to have a peak P_A indistinguishable from 1 [20]. The peak current responses to individual drugs and drug combinations were analyzed using the two-state (Resting-Active) concerted transition model [21, 22]. The concentration-response curves for (+)-catharanthine, loreclezole, and R(+)-etomidate were fitted, separately for each oocyte, to the state function:

$$P_A = \frac{1}{1 + L\left[\frac{1 + [drug]/K_{drug}}{1 + [drug]/\left(K_{drug} c_{drug}\right)}\right]^N} \quad (1)$$

where L is calculated as $(1\text{-}P_{A,background})/P_{A,background}$, and $P_{A,background}$ is the probability of being in the active state in the presence of a low concentration of GABA (P_A = 0.15–0.25) or the probability of being constitutively active [P_A = 0.00012 in wild-type [20]; P_A = 0.22 in β2(K279A)]. K_{drug} is the equilibrium dissociation constant for (+)-catharanthine, loreclezole or R(+)-etomidate in the resting receptor, c_{drug} is the ratio of the K_d for the drug in the active receptor to K_{drug}, [drug] is the concentration of the drug under study, and N is the number of binding sites.

To determine the type of interaction (steric *vs* allosteric) between (+)-catharanthine and R(+)-etomidate or loreclezole, the predicted peak responses were calculated using two models. First, a prediction was made assuming pure energetic additivity using Eq. (1). In this model, each drug interacts with a distinct set of binding sites, and one drug acts by increasing $P_{A,background}$ (reducing L) at which the response to the other drug is measured. In the second model, predictions were made assuming that the paired agents compete for common or overlapping binding sites. The predicted peak responses in this model were calculated using Eq. (2):

$$P_A = \frac{1}{1 + L\left[\frac{1 + [drug1]/K_{drug\ 1} + [drug2]/K_{drug\ 2}}{1 + [drug1]/\left(K_{drug1}\ c_{drug\ 1}\right) + [drug2]/\left(K_{drug\ 2} c_{drug\ 2}\right)}\right]^N} \quad (2)$$

where drug1 and drug2 denote R(+)-etomidate and (+)-catharanthine, or loreclezole and (+)-catharanthine, respectively, and N is the number of shared binding sites. Other terms are as described above. This approach has been described in detail previously [23].

When calculating the predicted P_A, the nominal concentrations of agonists or the values of c were adjusted to account for day-to-day variability to reflect the observed peak amplitudes in the presence of a single drug [23]. Thus, the predicted P_A of responses to drug combinations are calculated based on observed P_A responses to individual drugs rather than on their nominal concentrations. For example, the mean adjusted concentration of R(+)-etomidate in experiments examining receptor activation by the combination of R(+)-etomidate and (+)-catharanthine was 1.85 ± 0.31 μM, rather than the nominal 1 μM.

Modeling results were compared by calculating the difference in second-order Akaike information criterion scores of the two models [24, 25]:

Author Manuscript Author Manuscript Author Manuscript Author Manuscript

$$\Delta = n\ln\left(\frac{RSS_{Model\ 1}}{n}\right) - n\ln\left(\frac{RSS_{Model\ 2}}{n}\right) \quad (3)$$

where n is the number of oocytes, RSS is the residual sum of squares, and Models 1 and 2 refer to models considering distinct sites and shared sites, respectively. Akaike weights (w) for each model were then calculated as:

$$w_{distinct\ sites} = \frac{\exp\left[-\frac{1}{2}\Delta\right]}{\exp\left[-\frac{1}{2}\Delta\right] + 1} \quad (4)$$

and

$$w_{shared\ sites} = 1 - w_{distinct\ sites} \quad (5)$$

2.5. Statistical Analysis

Experimental data (mean ± SEM) were analyzed using Prism (GraphPad 6 or 8, Software Inc., La Jolla, CA, USA) or Excel 2016 (Microsoft, Redmond, WA, USA) software. Curve fitting was performed using Origin 2020 (OriginLab Corp., Northampton, MA, USA). Two-way ANOVA followed by Holm-Sidak's multiple comparisons tests were used to compare $GABA_AR$ subunit composition and drug concentration. Student's t-tests corrected by two comparisons were used to determine the effect of residue mutation on drug activity.

2.6. Molecular docking and molecular dynamics of (+)-catharanthine, R(+)-etomidate, and loreclezole using $GABA_AR$ models

The primary structures of the human α1, α2, β1, β2, β3, and γ2 $GABA_AR$ subunits were retrieved from the UniProt Consortium [26]. Subunit sequence alignment, model building, loop refinements, and quality evaluation procedures were performed by using the Prime module (v.5.5) of the Schrödinger Suite Release 2019-1 (Schrödinger, LLC, NY, USA). The structure of the α1β3γ2 $GABA_AR$ obtained by cryo-electron microscopy (PDB: 6HUJ) [15], corresponding to the picrotoxin/GABA-bound conformation, was used as a template in the homology modeling procedure. $GABA_AR$ models with single [i.e., β2(M286C), β2(N265S), β2(D282A), β2(R269A), or β2(K279A)], and double [i.e., β2(K279A+D282A)] mutations were prepared using the Protein Preparation Wizard tool implemented in the Schrödinger suite. The energy minimization protocol with a root mean square deviation (RMSD) value of 0.30 Å was applied using force field [27]. The ligand structures [i.e., (+)-catharanthine, R(+)-etomidate, and loreclezole] were prepared by Maestro (v.11.9) and evaluated for their ionization states at pH 7.4 ± 0.5 with Epik (v.4.7). The conjugate gradient method in Macromodel (v.12.3) was used for energy minimization (maximum iteration number: 2500; convergence criterion: 0.05 kcal/mol/$Å^2$).

For molecular docking of each ligand to different $GABA_AR$ models, the software Glide SP (v.8.2; default settings) was used. The grids were centered on the β(+)/α(−) interfacial site. The best pose for each compound was refined with Prime with a VSGB (Variable Surface

Author Manuscript Author Manuscript Author Manuscript Author Manuscript

Generalized Born) solvation model considering the target flexible within 3 Å around the ligand as previously described [28].

To determine the stability of the best docking poses for (+)-catharanthine and loreclezole in the studied $GABA_AR$ models, 100 ns molecular dynamics (MD) simulations were performed using Desmond Molecular Dynamics System (v.5.7) (Schrödinger suite) and OPL3e force field. Each receptor model, embedded in a model membrane of POPC (1-palmitoyl-2-oleoyl-sn-glycero-3-phosphocholine) (at 300 K), was solvated in an orthorhombic box using simple point charge water molecules extended 15 Å away from any protein atom around the TMD helices. The system was neutralized with 0.15 M Cl^- and Na^+. The simulation protocol included a starting relaxation step followed by a final production phase of 50 ns. In particular, the relaxation step comprised the following: (a) a stage of 100 ps at 10 K retaining the harmonic restraints on the solute heavy atoms (force constant of 50 kcal/mol/$Å^2$) using the NPT ensemble with Brownian dynamics; (b) a stage of 12 ps at 10 K with harmonic restraints on the solute heavy atoms (force constant of 50 kcal/mol/$Å^2$), using the NVT ensemble and Berendsen thermostat; (c) a stage of 12 ps at 10 K and 1 atm, retaining the harmonic restraints and using the NPT ensemble and Berendsen thermostat and barostat; (f) a stage of 12 ps at 300 K and 1 atm, retaining the harmonic restraints and using the NPT ensemble and Berendsen thermostat and barostat; (g) a final 24 ps stage at 300 K and 1 atm without harmonic restraints, using the NPT Berendsen thermostat and barostat. The final production phase of MD was run using a canonical NPT Berendsen ensemble at 300 K. During the MD simulation, a time step of 2 fs was used while constraining the bond lengths of H atoms with the M-SHAKE algorithm. The atomic coordinates of the system were saved every 100 ps along the MD trajectory. Protein RMSD, ligand RMSD/RMSF (Root Mean Square Fluctuation) ligand torsions evolution and occurrence of intermolecular H-bonds and hydrophobic contacts were provided by the Simulation Interaction Diagram implemented in Maestro along the production phase of the MD simulation. The tool reads the MD trajectory file and identifies ligand/target interactions repeatedly occurring during the simulation time. For instance, a 60% value suggests that the interaction is maintained for the 60% of the MD.

3. Results

3.1. (+)-Catharanthine-induced potentiation of GABA responses depends on the $GABA_AR$ subtype

To determine $GABA_AR$ subtype selectivity for the potentiating activity of (+)-catharanthine, electrophysiological recordings were performed on several ternary $\alpha_x\beta_y\gamma 2S$ $GABA_ARs$ (where x is 1–2; and y is 1–3). A representative tracing is shown in Fig. 2A. The results show that (+)-catharanthine potentiates GABA-induced currents in β2/3-containing receptors with higher efficacy compared to β1-containing receptors (Fig. 2B; Table 1), independently of whether the α subunit was the α1 or α2 isoform. Two-way ANOVA analyses showed a significant effect of receptor composition [$F(5,65) = 16.99$, $p < 0.0001$], (+)-catharanthine concentration [$F(2, 65) = 264.1$, $p < 0.0001$], and interaction between receptor composition and (+)-catharanthine concentration [$F(10,65) = 8.45$, $p < 0.0001$], indicating that (+)-catharanthine modulation is dependent on both its concentration

Author Manuscript Author Manuscript Author Manuscript Author Manuscript

and receptor composition. Holm-Sidak's multiple comparisons analysis indicated that (+)-catharanthine potentiation is higher at β2/3- than at β1-containing $GABA_AR$s ($p < 0.0001$).

Based on these results, we selected the β2-containing $GABA_AR$ for further characterization. Oocytes expressing α1β2γ2L $GABA_AR$s were exposed to 2 μM GABA ($P_A = 0.17 \pm 0.02$, n = 5 oocytes) in the absence or presence of 0.3–100 μM (+)-catharanthine. Sample current traces showing potentiation of GABA-elicited currents by 1, 10, or 100 μM (+)-catharanthine are shown in Fig. 3A. The figure also shows a current trace in the presence of 1 mM GABA + 50 μM propofol, illustrating the current level corresponding to P_A ~1, that was used to normalize the peak amplitudes in the presence of low GABA and low GABA + (+)-catharanthine (Fig. 3B). Fitting the concentration-response data to the Hill equation yielded an EC_{50} for potentiation by (+)-catharanthine of 13.5 ± 1.8 μM (mean ± SEM), a maximal efficacy [$(P_{Amax}/P_{Amin})-1 \times 100$] of 341 ± 53% of control (Table 1), and a Hill coefficient (n_H) of 1.66 ± 0.33. The fitted low-concentration asymptote had a P_A of 0.18 ± 0.02 (Fig. 3B).

Further analysis was conducted using a two-state concerted transition model [21, 22]. With the number of binding sites for (+)-catharanthine (N_{Cath}) tentatively constrained to 2 based on the estimated n_H, fitting the P_A data to (Eq. 1) yielded a K_{Cath} [i.e., K_d of (+)-catharanthine in the resting state] of 29.4 ± 6.0 μM and a c_{Cath} [ratio of K_ds of (+)-catharanthine in the active and resting states] of 0.231 ± 0.023 (Table 3). The binding of two (+)-catharanthine molecules thus contributes −1.76 kcal/mol free energy change to stabilize the active state, which is similar to that provided by the steroid allopregnanolone [23]. The estimated free energy change contributed by (+)-catharanthine is independent of the number of imposed binding sites, however, the value of c_{Cath} scales with N_{Cath} through the observed maximal P_A as: $P_{A,max} = 1/(1+Lc^N) = 1/(1+Lc^{'N'})$.

3.2. (+)-Catharanthine-induced $GABA_AR$ potentiation is sensitive to the β2(N265S) mutation but not the β3(M286C) or α1(Q241L) mutation

The involvement of previously identified binding sites for allosteric ligands in potentiation by (+)-catharanthine was investigated by testing selected mutations that affect receptor modulation by R(+)-etomidate, loreclezole, or potentiating neurosteroids. The underlying assumption in these experiments was that the mutations act locally and that involvement of a particular binding site in the actions of (+)-catharanthine will manifest as altered potentiation in the mutant receptor.

To determine the potential involvement of the R(+)-etomidate site in (+)-catharanthine's activity, we employed the β3(M286C) mutation that abolishes receptor potentiation by R(+)-etomidate [29]. Representative traces of GABA-induced currents are shown for the wild-type and mutant receptors in the absence and presence of (+)-catharanthine (Fig. 4A). Coapplication of 100 μM (+)-catharanthine enhanced the response to low (~EC_5) GABA by 667 ± 111% (n = 6 oocytes) in oocytes expressing the wild-type α1β3γ2S $GABA_AR$, and by 651 ± 115% (n = 5 oocytes) in oocytes expressing the α1β3(M286C)γ2S mutant. The data are summarized in Fig. 4A. In control experiments (not shown), 1 μM R(+)-etomidate potentiated the responses to low GABA by 376 ± 33% or 7 ± 3% (n = 5 oocytes for both) in oocytes expressing the wild-type or mutant receptors, respectively. Student's t-test analyses

Author Manuscript Author Manuscript Author Manuscript Author Manuscript

corrected by two comparisons indicated that the β3(M286C) mutation does not affect the positive modulation elicited by (+)-catharanthine ($t = 0.1007$, $df = 9$; $p > 0.05$) but decreases, as expected [29], receptor potentiation by R(+)-etomidate ($t = 10.18$, $df = 9$; $p < 0.001$).

Next, we tested the effect of (+)-catharanthine in the receptor containing the β2(N265S) mutation that has previously been reported to decrease receptor potentiation by loreclezole and R(+)-etomidate [30, 31]. Representative traces of GABA-induced currents in the absence and presence of 100 μM (+)-catharanthine for the wild-type and mutant receptors are shown in Fig. 4B. In oocytes expressing the wild-type α1β2γ2S receptor, 100 μM (+)-catharanthine potentiated the response to low (~EC_5) GABA by 1099 ± 163%. In contrast, (+)-catharanthine potentiated the response to GABA in oocytes expressing the α1β2(N265S)γ2S receptor by only 224 ± 13%. The data are summarized in Fig. 4B. In control experiments (not shown), 10 μM loreclezole potentiated the responses to low GABA by 269 ± 46% (n = 5 oocytes) in α1β2γ2S receptors, but only by 36 ± 6 % in α1β2(N265S)γ2S receptors (n = 4 oocytes). Student's t-test analyses corrected by two comparisons indicated that the β2(N265S) mutation affected both the positive modulation elicited by (+)-catharanthine ($t = 5.096$, $df = 11$; $p < 0.001$) and by loreclezole ($t = 4.474$, $df = 7$; $p < 0.01$).

To assess the involvement of a neurosteroid binding site located in the β(+)/α(−) interface but nearer to the cytoplasmic side of the membrane [32, 33], we examined potentiation by (+)-catharanthine in the receptor containing the α1(Q241L) mutation. This mutation has been reported to abolish or drastically decrease receptor potentiation by a variety of steroids including the neurosteroid allopregnanolone [32, 34, 35]. Coapplication of 30 μM (+)-catharanthine potentiated GABA-evoked currents in the α1β2γ2L $GABA_AR$ (2 μM GABA; $P_A = 0.15 \pm 0.02$) by 372 ± 72%, and in α1(Q241L)β2γ2L mutant $GABA_AR$ (30 μM GABA; $P_A = 0.19 \pm 0.05$) by 231 ± 33% (Fig. 4C). Student's t-test analysis indicated that the observed difference is not statistically significant ($p > 0.05$; n = 6 oocytes for each receptor). This finding is indicative of lack of involvement of the neurosteroid binding site in the β(+)/α(−) interface in mediating potentiation by (+)-catharanthine.

3.3. (+)-Catharanthine does not compete with R(+)-etomidate or the neurosteroid pregnanolone

In the next set of experiments, we employed a functional competition assay to determine whether (+)-catharanthine and R(+)-etomidate or loreclezole bind to overlapping or distinct sites. To determine whether the sites for (+)-catharanthine and R(+)-etomidate are overlapping, we measured receptor activation in the presence of R(+)-etomidate alone or in combination with (+)-catharanthine, and compared the observed P_A values with predictions made using activation models in which the drugs interact with unique or the same binding sites. In 7 oocytes expressing the wild-type α1β2γ2L receptor, the application of 1 μM R(+)-etomidate generated a response with a P_A of 0.035 ± 0.010. Coapplication of 10 μM (+)-catharanthine with R(+)-etomidate enhanced the P_A to 0.086 ± 0.024. Sample current traces are shown in Fig. 5A. In the model in which (+)-catharanthine and R(+)-etomidate interact with unique, non-overlapping sites, the expected potentiating effect of (+)-catharanthine could be calculated based on its activation parameters estimated in the

Author Manuscript Author Manuscript Author Manuscript Author Manuscript

presence of GABA (see section 3.1), and a modified L that expresses background activity arising from receptor activation by R(+)-etomidate. Using (Eq. 1), we calculated that the predicted P_A for the combination of 1 μM R(+)-etomidate + 10 μM (+)-catharanthine is 0.115 ± 0.031.

In the model in which (+)-catharanthine and R(+)-etomidate interact with the same or overlapping sites, the expected potentiation is based on competition between the two drugs and is sensitive to their relative efficacies. As the first step, we measured α1β2γ2L $GABA_AR$ activation in the presence of 1–300 μM R(+)-etomidate. The peak responses were converted to units of P_A and analyzed using Eq. (1). We estimated a K_{Eto} of 17.4 ± 4.9 μM [K_d for R(+)-etomidate in the resting state] and a c_{Eto} of 0.0060 ± 0.0004 (n = 6 oocytes). These values are similar to previous estimates of K and *c* for R(+)-etomidate in the α1β2γ2L $GABA_AR$ [36]. Using Eq. (2), we then calculated that the predicted P_A for the combination of 1 μM R(+)-etomidate + 10 μM (+)-catharanthine in the model where the two drugs interact with overlapping sites is 0.024 ± 0.006. The predicted reduction of the peak response upon coapplication of (+)-catharanthine with R(+)-etomidate in this model is due to (+)-catharanthine having lower efficacy (c_{Cath} = 0.231 *vs* c_{Eto} = 0.0060) that results in competitive inhibition by (+)-catharanthine. For quantitative comparison of the goodness of fit for both models, we calculated Akaike weights (*w*) that express the probability or likelihood that a particular model better describes the data [24, 25]. For the R(+)-etomidate + (+)-catharanthine combination, the $w_{distinct\ sites}$ was 0.995 and the $w_{shared\ sites}$ 0.005, indicating that these ligands bind to distinct, non-overlapping, sites.

Comparison of (+)-catharanthine-mediated potentiation of $GABA_ARs$ activated by R(+)-etomidate or GABA can provide qualitative insight into functional overlap and/or allosteric interactions between binding sites. It may be expected that for the ligand pairs R(+)-etomidate + (+)-catharanthine, and GABA + (+)-catharanthine, the degree of potentiation is similar if the nature of the interaction, i.e., lack of functional overlap or allosteric interaction between the sites, is similar [23]. Coapplication of 10 μM (+)-catharanthine potentiated the peak response elicited by 1 μM R(+)-etomidate (P_A = 0.035; above) by 160 ± 24% (n = 7 oocytes). Receptors activated by 1–2 μM GABA (P_A = 0.030 ± 0.007) were potentiated by 353 ± 68% (n = 5 oocytes) in the presence of (+)-catharanthine. Although the difference in mean potentiation is statistically significant (p = 0.012), it is relatively small and not supportive of a model in which the high-efficacy PAM R(+)-etomidate and the low-efficacy PAM (+)-catharanthine compete for a common binding site, and where the coapplication of (+)-catharanthine is expected to reduce the peak response to R(+)-etomidate. Sample current traces showing responses to R(+)-etomidate or GABA in the absence and presence of (+)-catharanthine are given in Fig. 5A. The data are summarized in Fig. 5B.

We also compared (+)-catharanthine-mediated potentiation of α1β2γ2L $GABA_ARs$ activated by the neurosteroid pregnanolone or GABA. In five oocytes, coapplication of 10 μM (+)-catharanthine potentiated the peak response to 2 μM pregnanolone (P_A = 0.005 ± 0.002) by 2200 ± 400%. The large degree of potentiation in these experiments is due to a relatively low P_A of the control response to the low-efficacy steroid. For comparison, receptors activated by 0.05 μM GABA (P_A = 0.004 ± 0.001) were potentiated by 1600 ± 400% (n = 5 oocytes). The effects are not significantly different (p > 0.05; t-test) supporting

Author Manuscript Author Manuscript Author Manuscript Author Manuscript

the notion that (+)-catharanthine and neurosteroids interact with distinct binding sites. Sample current traces showing potentiation of steroid vs. GABA-activated receptors are shown in Fig. 5C. The data are summarized in Fig. 5D.

3.4. (+)-Catharanthine competes with loreclezole

We next examined functional competition between (+)-catharanthine and loreclezole. To that end, we first measured loreclezole-induced potentiation of α1β2γ2L $GABA_A$Rs activated by a low concentration of GABA (10 μM; P_A = 0.26 ± 0.03; n = 6 oocytes). The concentration-response relationship fitted to the Hill equation yielded an EC_{50} of 3.4 ± 0.6 μM and a n_H of 1.27 ± 0.41, which are similar to previously reported values [37]. The peak responses were converted to units of P_A and analyzed using Eq. (1) as described above. We estimate a K_{Lor} (K_d for loreclezole in the resting state) of 7.1 ± 2.0 μM and a c_{Lor} of 0.251 ± 0.049 (n = 6 oocytes).

Because both (+)-catharanthine and loreclezole are weak agonists at $GABA_A$Rs, with *c* values of 0.225 and 0.251, respectively, no meaningful current response is expected when the compounds are applied alone or in combination. We therefore conducted the functional competition tests in the presence of a low concentration of GABA. Each oocyte was exposed to 0.2–0.5 μM GABA, GABA + 3 μM loreclezole, GABA + 30 μM (+)-catharanthine, and the combination of GABA + loreclezole + (+)-catharanthine. Sample current traces for each condition are shown in Fig. 5E. To establish the reference P_A ~1, each oocyte was also tested with 1 mM GABA + 50 μM propofol.

The mean P_A of the peak response to GABA alone was 0.009 ± 0.008 (n= 7 oocytes), whereas coapplication of loreclezole or (+)-catharanthine with GABA increased the P_A to 0.08 ± 0.05 or 0.16 ± 0.11, respectively. The P_A in the presence of GABA + loreclezole + (+)-catharanthine was 0.21 ± 0.13. The distinct site model, in which loreclezole and (+)-catharanthine bind to unique sites, predicts a P_A of 0.62 ± 0.17, whereas the same site model predicts a P_A of 0.19 ± 0.11 for the combination of GABA + loreclezole + (+)-catharanthine. The Akaike weights are ($1–10^{-9}$) and 10^{-9} for the same site and distinct site models, respectively, suggesting that loreclezole and (+)-catharanthine act through overlapping sites.

We also compared potentiation of R(+)-etomidate- and GABA-activated α1β2γ2L $GABA_A$Rs by loreclezole. Fig. 5F shows representative traces of loreclezole-induced potentiation of R(+)-etomidate- and GABA-activated receptors. We reasoned that if the binding site for loreclezole overlaps with that for R(+)-etomidate, then coapplication of the two compounds should generate a smaller response than when R(+)-etomidate is applied alone because the low-efficacy PAM loreclezole acts as a competitive inhibitor at the shared site. Loreclezole-induced potentiation of GABA-activated $GABA_A$Rs served as control for the degree of potentiation when loreclezole is combined with a drug that binds to a known distinct site. Coapplication of 10 μM loreclezole enhanced the peak response from receptors activated by 1 μM R(+)-etomidate (P_A = 0.039 ± 0.007) by 395 ± 48 %. For comparison, when $GABA_A$Rs were activated by 0.75 μM GABA (P_A = 0.051 ± 0.018), 10 μM loreclezole potentiated the peak response by 643 ± 91%. The finding that loreclezole potentiates, rather than inhibits, currents elicited by R(+)-etomidate indicates that the two compounds do not interact with overlapping sites. We note, however, that

Author Manuscript Author Manuscript Author Manuscript Author Manuscript

the difference between loreclezole-potentiation of R(+)-etomidate- and GABA-activated $GABA_A$Rs (395% vs. 643%) is statistically significant ($p = 0.038$) (Fig. 5G), indicating lack of full independence of the actions of loreclezole and R(+)-etomidate. It is plausible that the small reduction in the ability of loreclezole to potentiate R(+)-etomidate- *vs* GABA-activated receptors is a result of physical closeness of bound R(+)-etomidate and loreclezole in the β(+)/α(−) interface.

3.5. Molecular docking and molecular dynamics of (+)-catharanthine, R(+)-etomidate, and loreclezole to $GABA_A$R models

We built a homology model (HM) of the α1β2γ2 $GABA_A$R using the human α1β3γ2L structure (PDB: 6HUJ) [15] as the molecular template. After the development of the HMs and study of the putative location of the ligand binding region had already been completed, a cryo-EM-solved structure of the human α1β2γ2 $GABA_A$R in complex with R(+)-etomidate was published (PDB: 6X3V) [38]. We have used this structure to evaluate our *in silico* predictions. Fig. 6A shows the superposition of 6X3V and the adduct formed by etomidate docked within the HM. The docking protocol successfully predicted the binding mode of R(+)-etomidate both within 6X3V (RMSD value for nonhydrogen atoms of 0.4887 Å, Fig. 6B) and within the HM (RMSD value of 0.6062 Å for nonhydrogen atoms, Fig. 6C). In both ligand/target adducts, R(+)-etomidate binds at the β2-α1 interfaces with its phenyl ring packing against β2-N265, with an electrostatic interaction between the amide nitrogen of the side chain and the π electrons of the aromatic ring. The imidazole ring of R(+)-etomidate is sandwiched between β2-F289 and α-P333. Extensive van der Waals contacts are made at the interface, including with the side chain of β2-M286.

The molecular docking of (+)-catharanthine and loreclezole was characterized in different $GABA_A$R HMs, including α2β1γ2, α1β2γ2, and α2β3γ2, to determine the relevance of β_y and α_x subunits in these interactions. The amino acid sequence of the α1 and α2 subunits has 100% identity in the TM1-TM2 domains, while the β1 and β2/3 subunits differ by only two residues, (1) β2/3-N265, located in TM2, homologous to β1-S265, and (2) β2/3-M283, located in TM3, corresponding to β1-I283. To investigate the role of β2/3 residues at positions N265, M286, R269, D282, and K279 in ligand interactions, the α1β2(N265S)γ2, α1β2(M286C)γ2, α1β2(R269A)γ2, α1β2(D282A)γ2, α1β2(K279A)γ2, and α1β2(K279A+D282A)γ2 mutant receptors were constructed. The β2/3-N265 residue was replaced by S265 in wild-type β1 and mutant β2(N265S) subunits. The docking mode for each ligand was determined in the α1β2γ2 $GABA_A$R as a model of β2/3-containing receptors and subsequently compared to that found in the α2β1γ2 $GABA_A$R as a model of α1/2β1-containing receptors.

Outcomes from molecular docking carried out using the α1β2γ2 $GABA_A$R model indicated that (+)-catharanthine and loreclezole interact with a domain located within the β(+)/α(−) interface (Fig. 7A). The molecular docking of R(+)-etomidate correctly identified this domain as its binding site [38]. The site for (+)-catharanthine was found to be closer to the extracellular-transmembrane domain (ECD-TMD) junction (Fig. 7B), partially overlapping the loreclezole site, located in the non-luminal side of the TMD (Fig. 7B), whereas R(+)-etomidate site was located deeper in the TMD, partially overlapping the loreclezole (Fig.

Author Manuscript Author Manuscript Author Manuscript Author Manuscript

7C), but not (+)-catharanthine (Fig. 7B), binding area. MD simulations indicated that the stability of each ligand is greater in the β2-containing $GABA_AR$ model than that in the β1-containing $GABA_AR$ model.

The binding of (+)-catharanthine was stabilized by four H-bonds. The tertiary amine N atom and the indolic NH of the alkaloid formed H-bonds with the β2-R269 (TM2) side chain NH_2 group and with the β2-D282 (TM3) side chain carboxylic moiety, respectively (Fig. 8A; Table 2). Another two H-bonds were observed between the C=O and the O atoms of the ligand's methyl ester and the NH_2 of β2-N265 (TM2) and β2-K279 (TM2-TM3 loop), respectively. The stability of the observed H-bonds was maintained during most of the MD course in the wild-type α1β2γ2 (Fig. 8G). However, each mutant lost the capability of forming its own H-bond (Figs. 8B–F). In the case of the β2(N265S) mutation, even though Ser can form a H-bond, it is shorter than Asp, consequently the distance and the binding geometry were not optimal for the formation of a H-bond with (+)-catharanthine. Each mutation also decreased the stability of the other three H-bonds. For example, the β2(N265S) mutation decreased (+)-catharanthine interactions with R269 (from 73% to 60%), D282 (from 61% to 42%), and K279 (from 68% to 45%).

A wide network of hydrophobic interactions was also observed between the indole-azepinic ring of (+)-catharanthine and α1-TM1 (i.e., I228 and Q229) and β2-TM3 (i.e., D282 and L285) residues as well as between the tricycle and α1-Y225 aromatic ring (pre-TM1), the methyl ester and β2-L268/L272 (TM2), and the ethyl moiety and β2-P273/K274 (TM2-TM3 loop) (Fig. 8A; Table 2). (+)-Catharanthine could not form the respective H-bonds with A282 and A279 when the α1β2(D282A+K279A)γ2 double mutant was used (Fig. 8F; Table 2). As a result of the double mutation, a conformational rearrangement of the ligand within the binding pocket was produced, allowing the tricycle moiety to be accommodated in a wider hydrophobic area and the indolic and carboxymethyl groups forming new interactions (H-bond and π-cation) with β2-N265, β-R269, and α1-Q229 (Fig. 8F; Table 2). This rearrangement was observed in the very early stage of the MD simulation, and this new pose remained thereafter stable (Fig. 8G). The *in silico* mutational results clearly showed that H-bonds are important for (+)-catharanthine's stabilization within the binding pocket, where the double mutation induced more profound changes, reflected by ~4-fold larger RMSD values, than that induced by each single mutation (Fig. 8G).

The dichlorophenyl ring of loreclezole engaged in π-π stacking interactions with β2-F289 (TM3), and established vdW interactions with α1-TM1 (i.e., I228, P233, and T237), α1-TM2 (i.e., T265 and L269), and β2-TM2 (i.e., V258 and T262) residues (Fig. 9A; Table 3). The ligand's haloolefine moiety also formed hydrophobic contacts with α1-P233 (TM1) and α1-L269 (TM2) side chains, whereas its triazole ring formed two H-bonds with the NH_2 side chains of the β2-N265 and β2-R269 residues (TM2). These two H-bonds were stable for practically (69% and 76%, respectively) the whole MD simulation (Fig. 9C), indicating that the ligand is stable in this binding area. In both α1β2γ2 (Table 2) and α1β2(N265S)γ2 (Fig. 9B) models, however, a partial loss of triazole interactions with α1-TM1 (i.e., I228, Q229, and P233) and β2-TM2 (i.e., N265) residues was observed, as determined by a decreased stability (from 69% to 55%) in the mutant (Fig. 9C), whereas the H-bond with β2-R269 was maintained (Table 2). Loreclezole did not interact with β2-M286; therefore,

Author Manuscript Author Manuscript Author Manuscript Author Manuscript

the interactions present in the wild-type receptor are retained in the β2(M286C) mutant (Table 2).

3.6. Functional effects of mutations to the putative (+)-catharanthine binding site

Molecular docking studies suggested that the binding of (+)-catharanthine is stabilized by interactions with the N265, R269, K279, and D282 residues in the β2 subunit. To confirm the functional role of these interactions, we mutated the residues to alanine (R269A, K279A, D282A) or serine (N265S), and determined the effects of amino acid substitutions on receptor activation by (+)-catharanthine. The mutated receptors were directly activated by 0.3–100 μM (+)-catharanthine (K279A) or activated by a low concentration of GABA (P_A ~0.2) in the presence of 0.3–100 μM (+)-catharanthine (all others). The effects of (+)-catharanthine in the α1β2(K279A)γ2L receptor were studied in the absence of GABA because the mutation markedly enhanced constitutive activity ($P_{A,constitutive}$ = 0.22 ± 0.04), that negated the need to use a background agonist. Sample current traces are provided in Figs. 10A–B. The data were analyzed using the cyclic Resting-Active concerted transition model [Eq. (1)], and, descriptively, by fitting the concentration-response data to the Hill equation. A summary of analysis is given in Table 3.

The major relevant finding is that several mutations reduced gating efficacy of (+)-catharanthine (increased c_{Cath}, Table 3). The strongest effect in the single mutants was observed with the D282A mutation that reduced the change in free energy provided by (+)-catharanthine by 1.21 kcal/mol. The next two mutations that most affected the free energy change provided by (+)-catharanthine were K279A and N265S (reduced by 0.72 and 0.64 kcal/mol, respectively). Combination of two mutations in the same β subunit (K279A+D282A) resulted in an almost complete loss of sensitivity to (+)-catharanthine (ΔG = −0.19 ± 0.01 kcal/mol). The β2(R269A) mutation was essentially without effect on gating by (+)-catharanthine (ΔΔG = 0.23 kcal/mol). The mutations had a relatively small effect on K_{Cath}, although there was a tendency towards higher affinity of the resting receptor to (+)-catharanthine, that is also reflected in reduced (+)-catharanthine EC_{50} in the single mutants (Table 3).

The (+)-catharanthine concentration response data and fits to (Eq. 1) are shown in Fig. 10C. The data are replotted in Fig. 10D at a common, fixed background P_A of 0.15 using the K_{Cath} and c_{Cath} values in Table 3. This approach provides a clearer demonstration of the relative effects of mutations, because the differences in $P_{A,background}$ in Fig. 10C affect the apparent efficacy of the drug and can obscure the effects of mutations.

4. Discussion

The main objective of the study was to characterize the putative binding site and molecular mechanism underlying the potentiating activity of (+)-catharanthine at $GABA_A$Rs. Electrophysiological experiments indicated that the potentiating activity of (+)-catharanthine is greater at β2/3- compared to β1-containing $GABA_A$Rs, but equivalent at α1- and α2-containing receptors. Molecular docking and molecular dynamics results corroborated the preference for β2/3 subunits. Sensitivity to the β-subunit isoform has been previously shown for other GABAergic drugs, including sedative-anesthetics and anticonvulsants [13, 14],

Author Manuscript Author Manuscript Author Manuscript Author Manuscript

suggesting that the activity of (+)-catharanthine may be mediated by interactions with these allosteric binding sites. Mutational experiments and functional competition assays indicate that the site for (+)-catharanthine overlaps with the binding site for loreclezole, but not with R(+)-etomidate or neurosteroid sites in the β(+)/α(−) interface.

Functional competition assays involve measurement of receptor activity in the presence of two or more combined active compounds. The underlying premise is that a combination of drugs that act through distinct sites and mechanisms has different functional effect compared to a combination of drugs that share a binding site. Combination of two agonists or potentiators that act through distinct sites generally leads to enhanced function, whereas combination of compounds acting through the same site has limited potentiating effect or even leads to inhibition depending on the relative efficacies of the combined drugs. Comparison of empirical data with effects calculated from each model provides insight into which mechanism better describes the data [23].

Our data indicate that exposure to (+)-catharanthine potentiates the response to a low concentration of R(+)-etomidate. Given that (+)-catharanthine is a lower efficacy agonist than R(+)-etomidate (c_{Cath} = 0.231, c_{Eto} = 0.0060), the observation that (+)-catharanthine potentiates, rather than competitively inhibits, the response to R(+)-etomidate is indicative of distinct sites and mechanisms for the two drugs. We note that this approach does not provide information about the location or distance between the binding sites; strictly, the findings demonstrate that the receptor can simultaneously bind both drugs. Comparison of (+)-catharanthine-induced potentiation of GABA- vs. R(+)-etomidate-activated receptors showed a small but statistically significant difference in the magnitude of potentiation. Given the proximity of the putative binding sites for (+)-catharanthine and R(+)-etomidate (Figs. 7 and 8), we interpret this as changes in local interactions between the β(+)/α(−) interface and the two drugs, possibly due to physical closeness of the two bound ligands.

Activation of the receptor in the presence of the combination of (+)-catharanthine and loreclezole showed that the receptor can at any given time bind one but not both drugs. We interpret this finding as (+)-catharanthine and loreclezole binding to common or overlapping binding sites. While the caveat to this interpretation is that (+)-catharanthine could be allosterically modulating the binding of loreclezole, the sensitivity of the actions of both drugs to the β2(N265S) mutation in the β(+)/α(−) interface supports our conclusion. A recent study indicated that loreclezole binds with high affinity to the α(+)/β(−) interface in addition to the β(+)/α(−) intersubunit interface [39]. The gating efficacy of loreclezole at the α(+)/β(−) site, that would be relevant to potentiation of $GABA_AR$ function and sedation, is unknown. It is, however, likely to be minimal considering that the β2(N265S) mutation in the β(+)/α(−) interface largely eliminates loreclezole-mediated potentiation whereas the reverse β1(S265N) mutation increases the potentiation to wild-type β2-like level [30, 31].

Our *in silico* mutational studies supported the importance of β2-N265 in interactions with loreclezole and (+)-catharanthine, whereas β2-M286 is significant only for the interaction with R(+)-etomidate as previously shown [38]. From functional competition, site-directed mutagenesis, and molecular docking studies, we propose a model where (+)-catharanthine and loreclezole interact with neighboring or partially overlapping binding

Author Manuscript Author Manuscript Author Manuscript Author Manuscript

surfaces located within the β(+)/α(−) interface. Our docking results suggest that loreclezole and (+)-catharanthine may form independent H-bonds with the common residues β2-N265 and α1-Q229. On the other hand, loreclezole, but not (+)-catharanthine, establishes π-π interactions with β2-F289, as well as lipophilic interactions with β2-V258, whereas only R(+)-etomidate makes contact with α1-I228, α1-M236 and β2-V290. Previous mutational studies have supported the functional role of α1-M236 for R(+)-etomidate and β2-F289 for loreclezole [40].

Since (+)-catharanthine was the only ligand that formed a H-bond with the β2-K279 and β2-D282 residues, additional mutagenesis experiments were performed using single and double amino acid substitutions that abolish the predicted H-bonds. The results showed that the mutations decrease the gating efficacy (increase c_{Cath}) of (+)-catharanthine with the following rank order: K279A+D282A > D282A > K279A > R269A. The double mutation almost completely abolishes (+)-catharanthine activity, with near additive effects arising from each mutant. With the exception of D282A, that reduced K_{Cath} (equilibrium dissociation constant in the resting state), none of the mutations statistically significantly modified the affinity of the resting receptor to (+)-catharanthine. Gating efficacy (the value of c_{Cath}) is expressed as the ratio of equilibrium dissociation constants for (+)-catharanthine in the active and resting states. An increase in c_{Cath} with minimal change in K_{Cath} indicates reduced affinity to the drug in the active state. This is in agreement with the interactions identified by *in silico* modeling and tested electrophysiologically being applicable to the active/desensitized channel (PDB: 6HUJ). We also note that gating-selective effects of mutations to the agonist binding site have been observed previously for the AChR activated by ACh [41] and the $GABA_AR$ activated by R(+)-etomidate [42] or benzodiazepines [43].

The reduction in gating efficacy did not lead to right-shifted potentiation curves in the mutant receptors (Table 3). In part, this is due to a trend towards higher affinity of the resting receptor to (+)-catharanthine that compensates for the rightward shift in EC_{50} due to reduced efficacy. In addition, the extent of shift in EC_{50} depends on the actual level of efficacy. For low-efficacy drugs, a change in the value of c predominantly manifests as a change in maximal P_A rather than in the midpoint of concentration-response curve [19].

Our mutational analysis is based on the assumption that the mutations act locally and directly rather than allosterically. This may not be true. Measuring the effects of mutations to intersubunit interfaces on sensitivity to anesthetics, Szabo and coworkers [44] showed that amino acid substitutions at TM2–15' and TM3–36' positions also affected potentiation by drugs binding to non-adjacent interfaces. Specifically, they showed that the β3(N265M) and β3(M286W) mutations at the β(+)/α(−) interface reduced potentiation by the barbiturate analog *m*TFD-MPAB that binds at the α(+)/β(−) and γ(+)/β(−) interfaces. In our hands, potentiation by (+)-catharanthine was unaffected by β3(M286C), indicating lack of direct or allosteric effects, but the gating efficacy of (+)-catharanthine was reduced in the β2(N265S) mutant. While the effect may not be direct given prior data on *m*TFD-MPAB [44], the involvement of this residue and the β(+)/α(−) interface are supported by *in silico* modeling and functional competition experiments. Analogous caveats apply to other tested mutants.

Author Manuscript Author Manuscript Author Manuscript Author Manuscript

To recapitulate, the major conclusion of this study is that (+)-catharanthine selectively potentiates β2/3- over β1-containing $GABA_AR$s, and that this activity is mediated by a site located within the β(+)/α(−)interface in the TMD, near the TM2-TM3 loop. The binding of (+)-catharanthine is stabilized by several H-bonds in a site that partially overlaps the loreclezole site, but not the R(+)-etomidate or the neurosteroid sites.

Acknowledgements

We thank A. Abou-Elazab and F. Steudle for excellent technical assistance, Sonia Mason for the oocyte harvesting, and Dr. Kuehne for supplying (+)-catharanthine hydrochloride.

Funding

This research was supported by National Institutes of Health (grants U24AA025479 to R.A.H.; R01GM108580 and R35GM140947 to G.A.); the Taylor Family Institute for Innovative Psychiatric Research (to G.A.), and OVPR Pilot/Seed Grants (OSU-CHS) (to H.R.A.).

Abbreviations:

AChR
nicotinic acetylcholine receptor

allopregnanolone
(PubChem CID: 92786)

(+)-catharanthine(+)-3,4-didehydrocoronaridine
(PubChem CID: 418553)

ECD
extracellular domain

GABA
γ-aminobutyric acid

$GABA_AR$
GABA type A receptor

HM
homology model

Kd
equilibrium dissociation constant

loreclezole
(PubChem CID: 3034012)

18-MC
18-methoxycoronaridine (PubChem CID: 10248465)

MD
molecular dynamics

Author Manuscript Author Manuscript Author Manuscript Author Manuscript

nH
Hill coefficient

P_A
probability of being in the active state

PAM
positive allosteric modulator

potentiating EC_{50}
ligand concentration that produces half-maximal potentiation response

pregnanolone1-[(1*S*,3a*S*,3b*R*,5a*R*,7*R*,9a*S*,9b*S*,11a*S*)-7-Hydroxy-9a,11a-dimethylhexadecahydro-1*H*-cyclopenta[*a*]phenanthren-1-yl]ethan-1-one
(PubChem CID: 31402)

R(+)-etomidate
(PubChem CID: 667484)

RMSD
root mean square deviation

TMD
transmembrane domain

References

[1]. Maisonneuve IM, Glick SD, Anti-addictive actions of an iboga alkaloid congener: a novel mechanism for a novel treatment, Pharmacol Biochem Behav 75(3) (2003) 607–18. [PubMed: 12895678]

[2]. Glick SD, Kuehne ME, Raucci J, Wilson TE, Larson D, Keller RW Jr., Carlson JN, Effects of iboga alkaloids on morphine and cocaine self-administration in rats: relationship to tremorigenic effects and to effects on dopamine release in nucleus accumbens and striatum, Brain Res 657(1–2) (1994) 14–22. [PubMed: 7820611]

[3]. Arias HR, Jin X, Feuerbach D, Drenan RM, Selectivity of coronaridine congeners at nicotinic acetylcholine receptors and inhibitory activity on mouse medial habenula, Int J Biochem Cell Biol 92 (2017) 202–209. [PubMed: 29042244]

[4]. Glue P, Cape G, Tunnicliff D, Lockhart M, Lam F, Hung N, Hung CT, Harland S, Devane J, Crockett RS, Howes J, Darpo B, Zhou M, Weis H, Friedhoff L, Ascending Single-Dose, Double-Blind, Placebo-Controlled Safety Study of Noribogaine in Opioid-Dependent Patients, Clin Pharmacol Drug Dev 5(6) (2016) 460–468. [PubMed: 27870477]

[5]. Brown TK, Alper K, Treatment of opioid use disorder with ibogaine: detoxification and drug use outcomes, Am J Drug Alcohol Abuse 44(1) (2018) 24–36. [PubMed: 28541119]

[6]. Rodríguez P, Urbanavicius J, Prieto JP, Fabius S, Reyes AL, Havel V, Sames D, Scorza C, Carrera I, A Single Administration of the Atypical Psychedelic Ibogaine or Its Metabolite Noribogaine Induces an Antidepressant-Like Effect in Rats, ACS Chem Neurosci 11(11) (2020) 1661–1672. [PubMed: 32330007]

[7]. Arias HR, Tae HS, Micheli L, Yousuf A, Ghelardini C, Adams DJ, Di Cesare Mannelli L, Coronaridine congeners decrease neuropathic pain in mice and inhibit alpha9alpha10 nicotinic acetylcholine receptors and $Ca_V2.2$ channels, Neuropharmacology 175 (2020) 108194. [PubMed: 32540451]

Author Manuscript Author Manuscript Author Manuscript Author Manuscript

[8]. Arias HR, Do Rego JL, Do Rego JC, Chen Z, Anouar Y, Scholze P, Gonzales EB, Huang R, Chagraoui A, Coronaridine congeners potentiate GABA-A receptors and induce sedative activity in mice in a benzodiazepine-insensitive manner, Prog Neuropsychopharmacol Biol Psychiatry 101 (2020) 109930. [PubMed: 32194202]

[9]. Jasmin L, Wu MV, Ohara PT, GABA puts a stop to pain, Curr Drug Targets CNS Neurol Disord 3(6) (2004) 487–505. [PubMed: 15578966]

[10]. Stephens DN, King SL, Lambert JJ, Belelli D, Duka T, GABAA receptor subtype involvement in addictive behaviour, Genes Brain Behav 16(1) (2017) 149–184. [PubMed: 27539865]

[11]. Greenfield LJ Jr., Molecular mechanisms of antiseizure drug activity at GABA-A receptors, Seizure 22(8) (2013) 589–600. [PubMed: 23683707]

[12]. Miller PS, Scott S, Masiulis S, De Colibus L, Pardon E, Steyaert J, Aricescu AR, Structural basis for GABA-A receptor potentiation by neurosteroids, Nat Struct Mol Biol 24(11) (2017) 986–992. [PubMed: 28991263]

[13]. Sieghart W, Savic MM, International Union of Basic and Clinical Pharmacology. CVI: GABA-A Receptor Subtype- and Function-selective Ligands: Key Issues in Translation to Humans, Pharmacol Rev 70(4) (2018) 836–878. [PubMed: 30275042]

[14]. Weir CJ, Mitchell SJ, Lambert JJ, Role of GABA-A receptor subtypes in the behavioural effects of intravenous general anaesthetics, Br J Anaesth 119(suppl_1) (2017) i167–i175. [PubMed: 29161398]

[15]. Masiulis S, Desai R, Uchanski T, Serna Martin I, Laverty D, Karia D, Malinauskas T, Zivanov J, Pardon E, Kotecha A, Steyaert J, Miller KW, Aricescu AR, GABA-A receptor signalling mechanisms revealed by structural pharmacology, Nature 565(7740) (2019) 454–459. [PubMed: 30602790]

[16]. Kuehne ME, Bornmann WG, Earley WG, Marko I, Studies in Biomimetic Alkaloid Syntheses .14. Controlled, Selective Syntheses of Catharanthine and Tabersonine, and Related Desethyl Compounds, through Generation of 15-Oxosecodine Intermediates, J Org Chem 51(15) (1986) 2913–2927.

[17]. Germann AL, Shin DJ, Manion BD, Edge CJ, Smith EH, Franks NP, Evers AS, Akk G, Activation and modulation of recombinant glycine and GABA(A) receptors by 4-halogenated analogues of propofol, Brit J Pharmacol 173(21) (2016) 3110–3120. [PubMed: 27459129]

[18]. Draguhn A, Verdorn TA, Ewert M, Seeburg PH, Sakmann B, Functional and molecular distinction between recombinant rat GABAA receptor subtypes by Zn2+, Neuron 5(6) (1990) 781–8. [PubMed: 1702644]

[19]. Akk G, Shin DJ, Germann AL, Steinbach JH, GABA Type A Receptor Activation in the Allosteric Coagonist Model Framework: Relationship between EC50 and Basal Activity, Mol Pharmacol 93(2) (2018) 90–100. [PubMed: 29150461]

[20]. Shin DJ, Germann AL, Steinbach JH, Akk G, The actions of drug combinations on the GABA-A receptor manifest as curvilinear isoboles of additivity, Mol Pharmacol 92(5) (2017) 556–563. [PubMed: 28790148]

[21]. Steinbach JH, Akk G, Applying the Monod-Wyman-Changeux Allosteric Activation Model to Pseudo-Steady-State Responses from GABA-A Receptors, Mol Pharmacol 95(1) (2019) 106–119. [PubMed: 30333132]

[22]. Forman SA, Monod-Wyman-Changeux allosteric mechanisms of action and the pharmacology of etomidate, Curr Opin Anaesthesiol 25(4) (2012) 411–8. [PubMed: 22614249]

[23]. Shin DJ, Germann AL, Covey DF, Steinbach JH, Akk G, Analysis of GABA-A Receptor Activation by Combinations of Agonists Acting at the Same or Distinct Binding Sites, Mol Pharmacol 95(1) (2019) 70–81. [PubMed: 30337372]

[24]. Wagenmakers EJ, Farrell S, AIC model selection using Akaike weights, Psychon Bull Rev 11(1) (2004) 192–6. [PubMed: 15117008]

[25]. Burnham KP, Anderson DR, Huyvaert KP, AIC model selection and multimodel inference in behavioral ecology: some background, observations, and comparisons, Behav Ecol Sociobiol 65(January 2011) (2011) 23–35.

[26]. UniProt C, UniProt: a worldwide hub of protein knowledge, Nucleic Acids Res 47(D1) (2019) D506–D515. [PubMed: 30395287]

Author Manuscript Author Manuscript Author Manuscript Author Manuscript

[27]. Roos K, Wu C, Damm W, Reboul M, Stevenson JM, Lu C, Dahlgren MK, Mondal S, Chen W, Wang L, Abel R, Friesner RA, Harder ED, OPLS3e: Extending Force Field Coverage for Drug-Like Small Molecules, J Chem Theory Comput 15(3) (2019) 1863–1874. [PubMed: 30768902]

[28]. Nocentini A, Gratteri P, Supuran CT, Phosphorus versus Sulfur: Discovery of Benzenephosphonamidates as Versatile Sulfonamide-Mimic Chemotypes Acting as Carbonic Anhydrase Inhibitors, Chemistry 25(5) (2019) 1188–1192. [PubMed: 30411821]

[29]. Ziemba AM, Szabo A, Pierce DW, Haburcak M, Stern AT, Nourmahnad A, Halpin ES, Forman SA, Alphaxalone Binds in Inner Transmembrane beta+-alpha- Interfaces of alpha1beta3gamma2 gamma-Aminobutyric Acid Type A Receptors, Anesthesiology 128(2) (2018) 338–351. [PubMed: 29210709]

[30]. Reynolds DS, Rosahl TW, Cirone J, O'Meara GF, Haythornthwaite A, Newman RJ, Myers J, Sur C, Howell O, Rutter AR, Atack J, Macaulay AJ, Hadingham KL, Hutson PH, Belelli D, Lambert JJ, Dawson GR, McKernan R, Whiting PJ, Wafford KA, Sedation and anesthesia mediated by distinct GABA-A receptor isoforms, J Neurosci 23(24) (2003) 8608–17. [PubMed: 13679430]

[31]. Wingrove PB, Wafford KA, Bain C, Whiting PJ, The modulatory action of loreclezole at the gamma-aminobutyric acid type A receptor is determined by a single amino acid in the beta2 and beta3 subunit, Proc Natl Acad Sci U S A 91(10) (1994) 4569–73. [PubMed: 8183949]

[32]. Hosie AM, Wilkins ME, da Silva HM, Smart TG, Endogenous neurosteroids regulate GABA-A receptors through two discrete transmembrane sites, Nature 444(7118) (2006) 486–9. [PubMed: 17108970]

[33]. Chen ZW, Bracamontes JR, Budelier MM, Germann AL, Shin DJ, Kathiresan K, Qian MX, Manion B, Cheng WWL, Reichert DE, Akk G, Covey DF, Evers AS, Multiple functional neurosteroid binding sites on GABA-A receptors, PLoS Biol 17(3) (2019) e3000157. [PubMed: 30845142]

[34]. Akk G, Li P, Bracamontes J, Reichert DE, Covey DF, Steinbach JH, Mutations of the GABA-A receptor alpha1 subunit M1 domain reveal unexpected complexity for modulation by neuroactive steroids, Mol Pharmacol 74(3) (2008) 614–27. [PubMed: 18544665]

[35]. Germann AL, Pierce SR, Tateiwa H, Sugasawa Y, Reichert DE, Evers AS, Steinbach JH, Akk G, Intrasubunit and Intersubunit Steroid Binding Sites Independently and Additively Mediate alpha1beta2gamma2L GABAA Receptor Potentiation by the Endogenous Neurosteroid Allopregnanolone, Mol Pharmacol 100(1) (2021) 19–31. [PubMed: 33958479]

[36]. Rüsch D, Zhong H, Forman SA, Gating allosterism at a single class of etomidate sites on alpha1beta2gamma2L GABA-A receptors accounts for both direct activation and agonist modulation, J Biol Chem 279(20) (2004) 20982–92. [PubMed: 15016806]

[37]. Wafford KA, Bain CJ, Quirk K, McKernan RM, Wingrove PB, Whiting PJ, Kemp JA, A novel allosteric modulatory site on the GABAA receptor beta subunit, Neuron 12(4) (1994) 775–82. [PubMed: 8161449]

[38]. Kim JJ, Gharpure A, Teng JF, Zhuang YX, Howard RJ, Zhu ST, Noviello CM, Walsh RM, Lindahl E, Hibbs RE, Shared structural mechanisms of general anaesthetics and benzodiazepines, Nature 585(7824) (2020) 303-+. [PubMed: 32879488]

[39]. Jayakar SS, Zhou X, Chiara DC, Jarava-Barrera C, Savechenkov PY, Bruzik KS, Tortosa M, Miller KW, Cohen JB, Identifying Drugs that Bind Selectively to Intersubunit General Anesthetic Sites in the alpha1beta3gamma2 $GABA_AR$ Transmembrane Domain, Mol Pharmacol 95(6) (2019) 615–628. [PubMed: 30952799]

[40]. Siegwart R, Krahenbuhl K, Lambert S, Rudolph U, Mutational analysis of molecular requirements for the actions of general anaesthetics at the gamma-aminobutyric acid(A) receptor subtype, alpha1beta2gamma2, BMC Pharmacol 3 (2003) 13. [PubMed: 14613517]

[41]. Akk G, Zhou M, Auerbach A, A mutational analysis of the acetylcholine receptor channel transmitter binding site, Biophys J 76(1 Pt 1) (1999) 207–18. [PubMed: 9876135]

[42]. Stewart D, Desai R, Cheng Q, Liu A, Forman SA, Tryptophan mutations at azi-etomidate photo-incorporation sites on alpha1 or beta2 subunits enhance GABAA receptor gating and reduce etomidate modulation, Mol Pharmacol 74(6) (2008) 1687–95. [PubMed: 18805938]

Author Manuscript Author Manuscript Author Manuscript Author Manuscript

[43]. Morlock EV, Czajkowski C, Different residues in the GABAA receptor benzodiazepine binding pocket mediate benzodiazepine efficacy and binding, Mol Pharmacol 80(1) (2011) 14–22. [PubMed: 21447642]

[44]. Szabo A, Nourmahnad A, Halpin E, Forman SA, Monod-Wyman-Changeux Allosteric Shift Analysis in Mutant alpha1beta3gamma2L GABAA Receptors Indicates Selectivity and Crosstalk among Intersubunit Transmembrane Anesthetic Sites, Mol Pharmacol 95(4) (2019) 408–417. [PubMed: 30696720]

Author Manuscript Author Manuscript Author Manuscript Author Manuscript

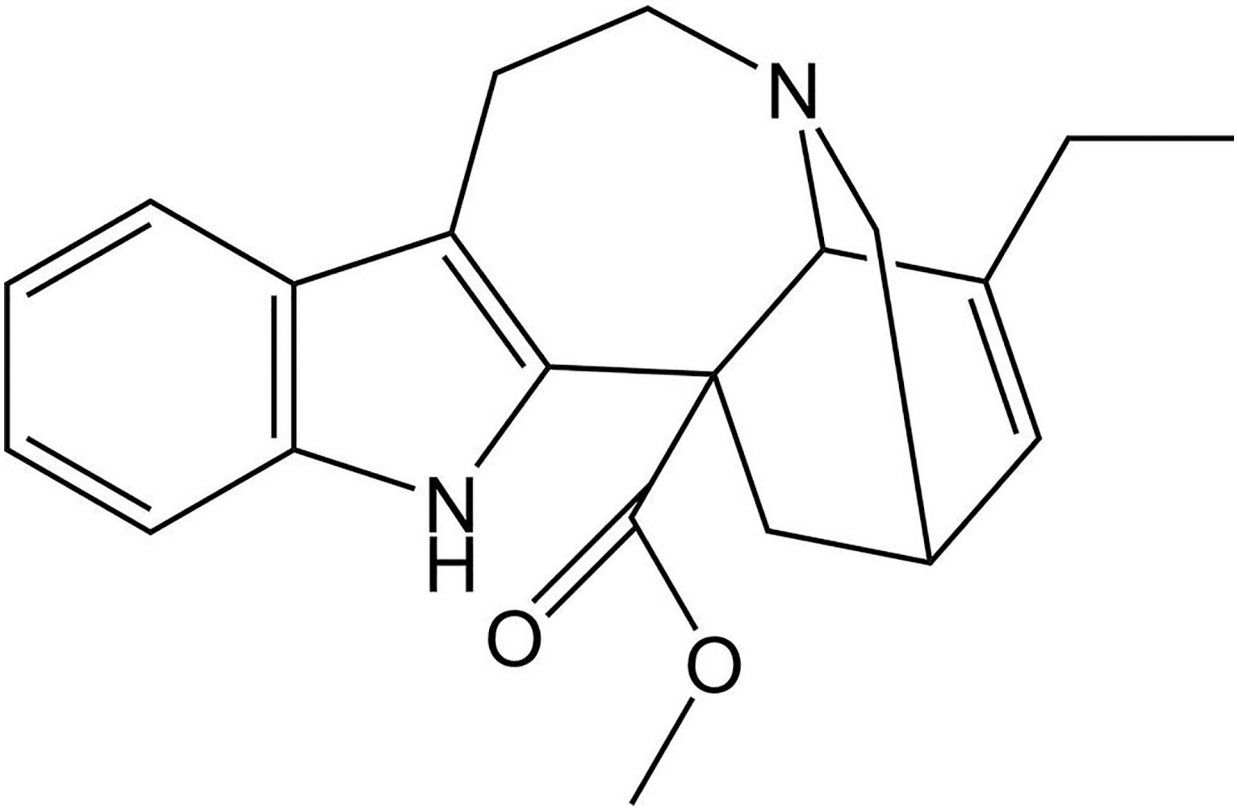

Figure 1.
(+)-Catharanthine structure. PubChem CID: 418553.

Author Manuscript Author Manuscript Author Manuscript Author Manuscript

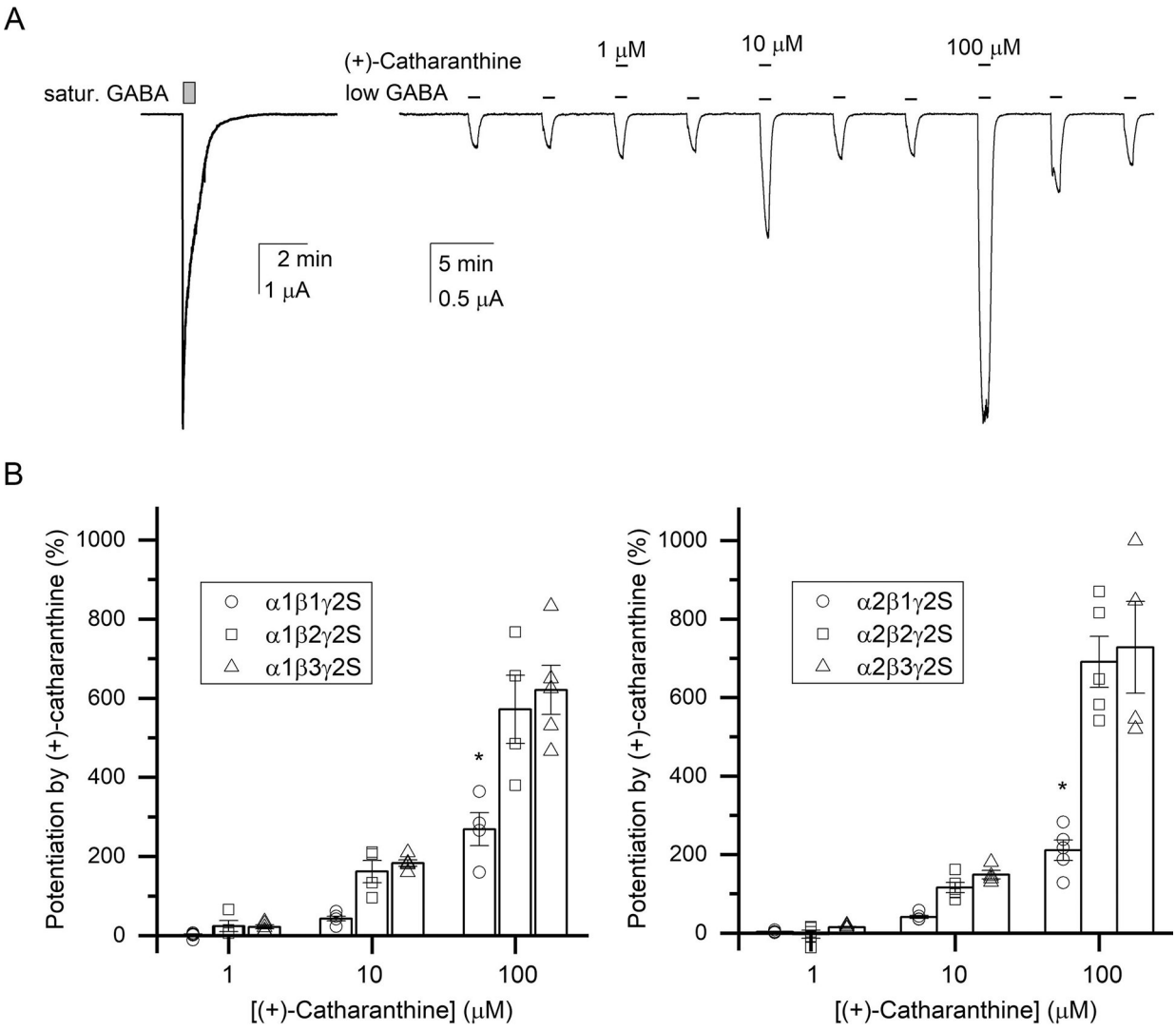

Figure 2.

(+)-Catharanthine-induced potentiation of subsaturating GABA responses at $GABA_AR$s expressed in *X. laevis* oocytes. (A) Representative EC_5 GABA (2 μM)-induced currents in α1β3γ2S $GABA_AR$s in the absence and presence of 1, 10, or 100 μM (+)-catharanthine, and a trace showing a response to 1 mM GABA in the same cell. The currents were recorded at −70 mV. (B) Summary of $GABA_AR$ potentiation by 1, 10, or 100 μM (+)-catharanthine. Data (n = 4–5 oocytes each) show the change of the GABA response as a percentage of the control GABA response [mean ± SEM of the EC_5 GABA before and after the co-application with (+)-catharanthine]. Two-way ANOVA followed by Holm-Sidak's multiple comparisons test analyses indicated that (+)-catharanthine-induced potentiation was higher at β2/β3- *vs* β1-containing $GABA_AR$s (*$p < 0.0001$), whereas no significant differences were observed between α1- and α2-containing $GABA_AR$s containing the same β subunit (the analysis was performed using all data but split in two graphs for clarity). The apparent potentiating efficacy of 100 μM (+)-catharanthine at each receptor subtype is summarized in Table 1.

Author Manuscript Author Manuscript Author Manuscript Author Manuscript

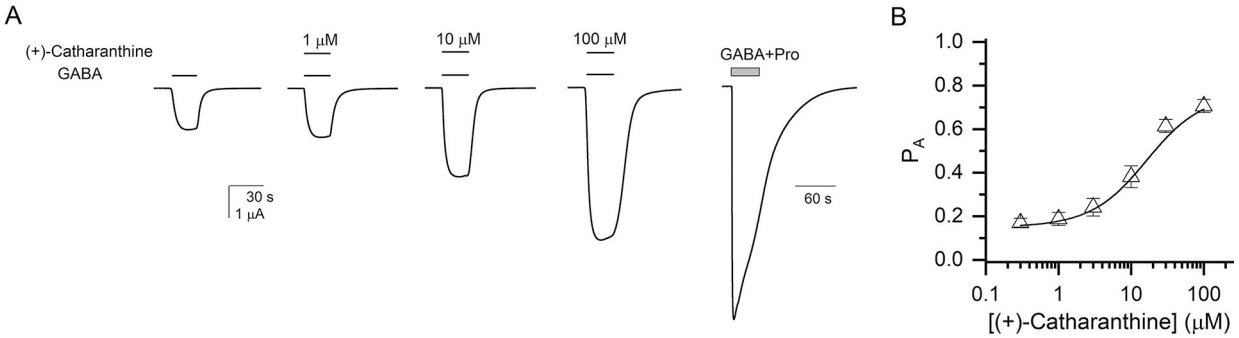

Figure 3.

(+)-Catharanthine potentiated α1β2γ2L $GABA_A$Rs expressed in *X. laevis* oocytes in a concentration-dependent manner. (A) Representative α1β2γ2L $GABA_A$R currents elicited by 2 μM GABA (P_A = 0.18) in the absence or presence of 1, 10, and 100 μM (+)-catharanthine, and a trace showing a response to 1 mM GABA + 50 μM propofol (GABA+Pro; peak P_A ~1). All responses are from the same oocyte. The currents were recorded at −60 mV. (B) Concentration-response relationship for potentiation of the α1β2γ2 $GABA_A$R by (+)-catharanthine. The peak responses to GABA + (+)-catharanthine were normalized to the peak response to 1 mM GABA + 50 μM propofol (P_A ~1) in the same cells. The data points give mean ± SEM from 5 oocytes. The curve represents a fit to (Eq. 1), yielding a K_{Cath} of 29.4 μM and a c_{Cath} of 0.231, with N_{Cath} constrained to 2 (Table 3). Fitting the concentration-response data to the Hill equation yielded an EC_{50} of 13.5 μM, a Hill coefficient of 1.66, and maximum potentiation of 341%.

Author Manuscript Author Manuscript Author Manuscript Author Manuscript

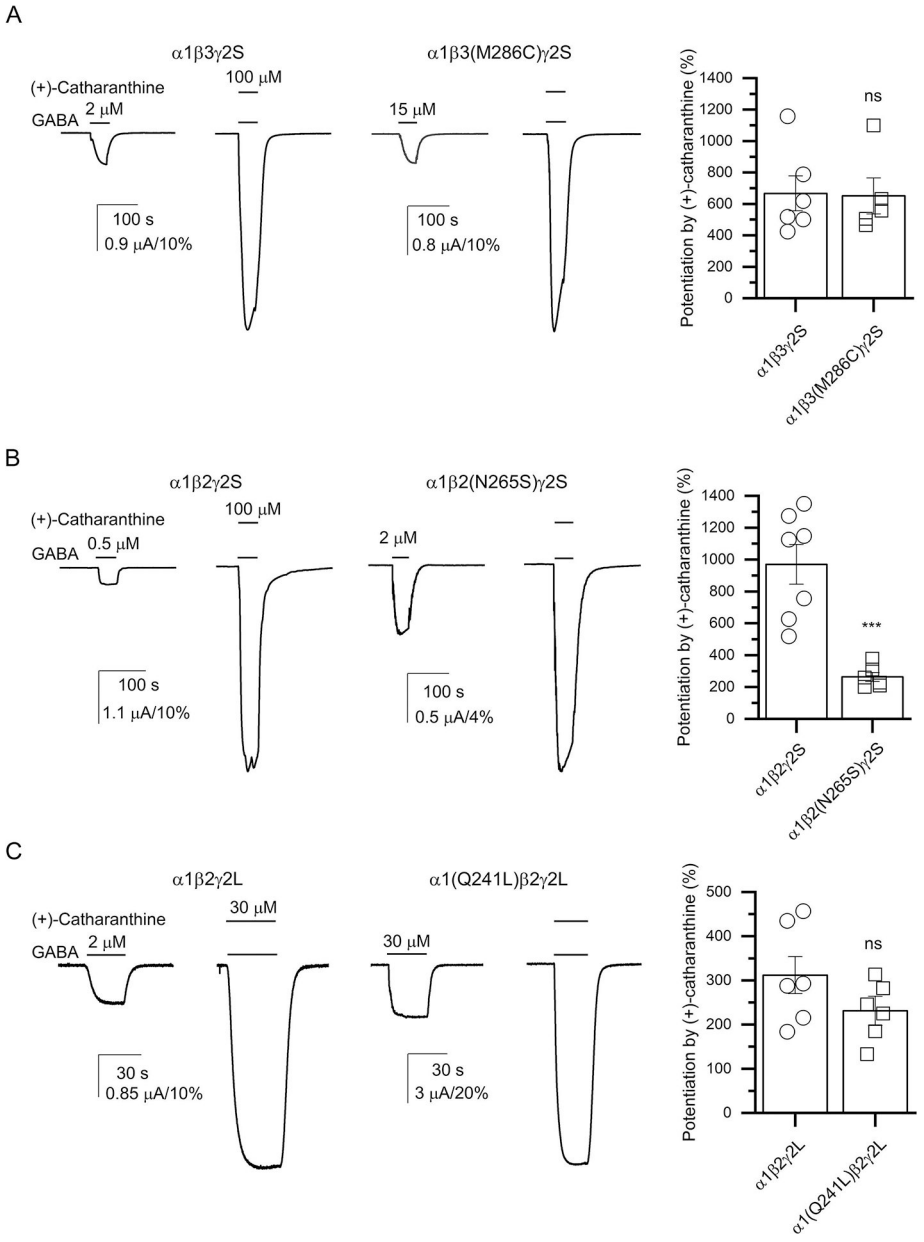

Figure 4.

The β2(N265S), but not the β3(M286C) or α1(Q241L), mutation, reduces (+)-catharanthine-induced potentiation. Representative current traces of wild-type or mutant receptors activated by (A) EC_5 GABA [2 μM GABA in α1β3γ2S wild-type and 15 μM GABA in β3(M286C) mutant]; (B) EC_5 GABA [0.5 μM GABA in α1β2γ2S wild-type and 2 μM GABA in β2(N265S) mutant], or (C) EC_{15} GABA [2 μM GABA in α1β2γ2L wild-type and 30 μM GABA in α1(Q241L) mutant], in the absence or presence of 100 μM (A and B) or 30 μM (+)-catharanthine (C). The calibration bars show current amplitude in μA, and in % of the peak response to saturating GABA for scaling purposes. The currents were recorded at −70 mV in A and B, and at −60 mV in C. A summary of wild-type and mutant receptor potentiation by (+)-catharanthine, expressed as mean ± SEM % change

Author Manuscript Author Manuscript Author Manuscript Author Manuscript

in GABA response, is shown next to the current traces. Student's t-test analysis indicated that the β2(N265S) mutation reduces potentiation by (+)-catharanthine ($p < 0.01$; $n = 6–7$ oocytes), whereas neither the β3(M286C) nor α1(Q241L) mutation affected potentiation by (+)-catharanthine ($p > 0.05$; $n = 5–6$ oocytes for each receptor).

Author Manuscript Author Manuscript Author Manuscript Author Manuscript

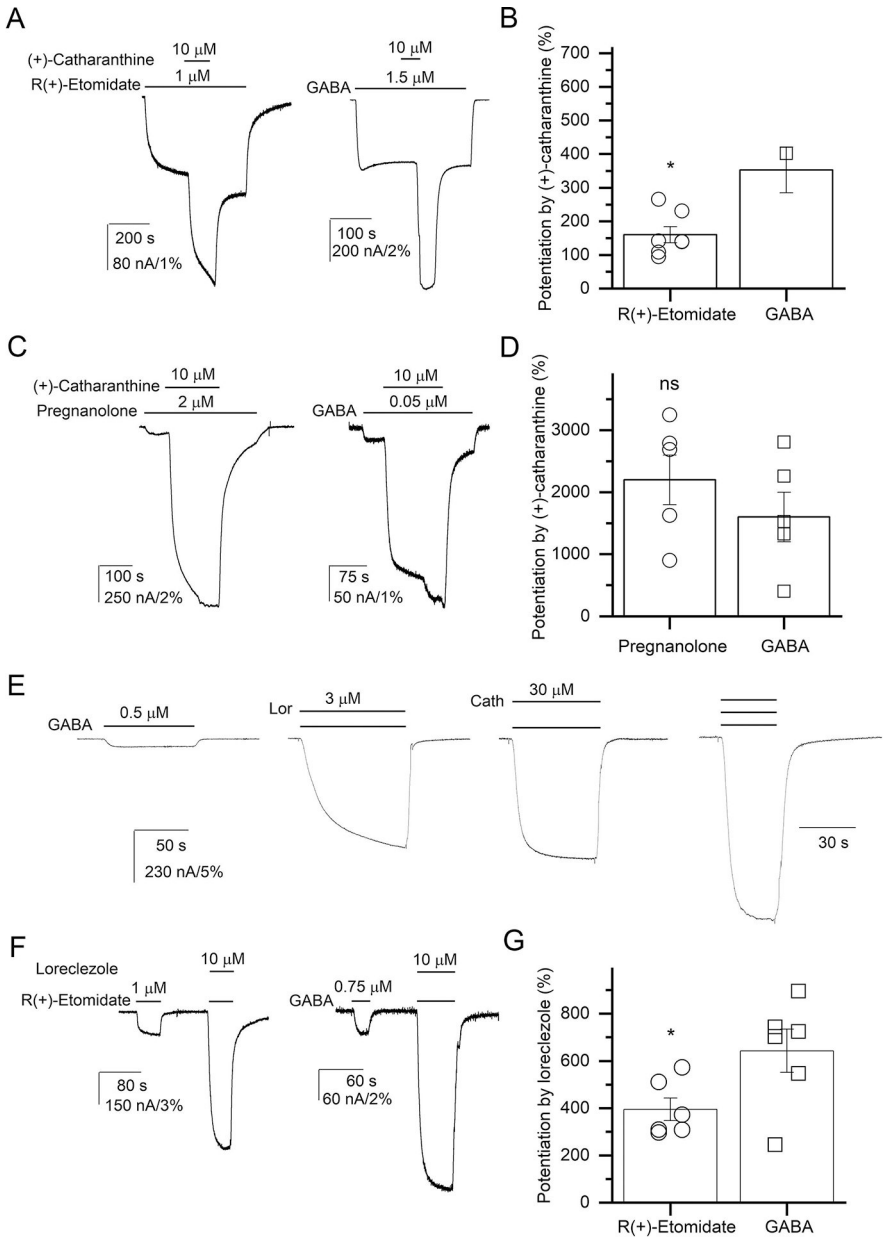

Figure 5.

Steric *vs* allosteric interactions between (+)-catharanthine and R(+)-etomidate, (+)-catharanthine and loreclezole, and R(+)-etomidate and loreclezole. (A) Sample traces showing potentiation of 1 μM R(+)-etomidate and 1.5 μM GABA-activated α1β2γ2L $GABA_A$Rs by 10 μM (+)-catharanthine. (B) Percent of change of R(+)-etomidate- or GABA-elicited responses by 10 μM (+)-catharanthine. Student's t-test analysis of data indicated that the observed change is statistically significantly ($p = 0.012$; $n = 5–6$ oocytes). (C) Sample traces showing potentiation of 2 μM pregnanolone and 0.05 μM GABA-activated α1β2γ2L $GABA_A$Rs by 10 μM (+)-catharanthine. (D) Percent of change of pregnanolone- or GABA-elicited responses by 10 μM (+)-catharanthine. Student's t-test analysis of data indicated that the observed change is statistically significantly ($p > 0.05$;

Author Manuscript Author Manuscript Author Manuscript Author Manuscript

n = 5 oocytes per agonist). (E) Sample traces showing activation of α1β2γ2 $GABA_A$Rs by 0.5 μM GABA, GABA + 3 μM loreclezole (Lor), GABA + 30 μM (+)-catharanthine (Cath), or GABA + loreclezole + (+)-catharanthine. (F) Sample traces showing potentiation of 1 μM R(+)-etomidate and 0.75 μM GABA-activated α1β2γ2 $GABA_A$Rs by 10 μM loreclezole. (G) Percent of change of R(+)-etomidate- or GABA-elicited responses by 10 μM loreclezole. Student's t-test analysis of data indicated that the observed change is statistically significant ($p = 0.038$; n = 6 oocytes for each receptor). All currents were recorded at −60 mV. The calibration bars show current amplitude in μA, and in % of the peak response to 1 mM GABA + 50 μM propofol for scaling purposes.

Author Manuscript Author Manuscript Author Manuscript Author Manuscript

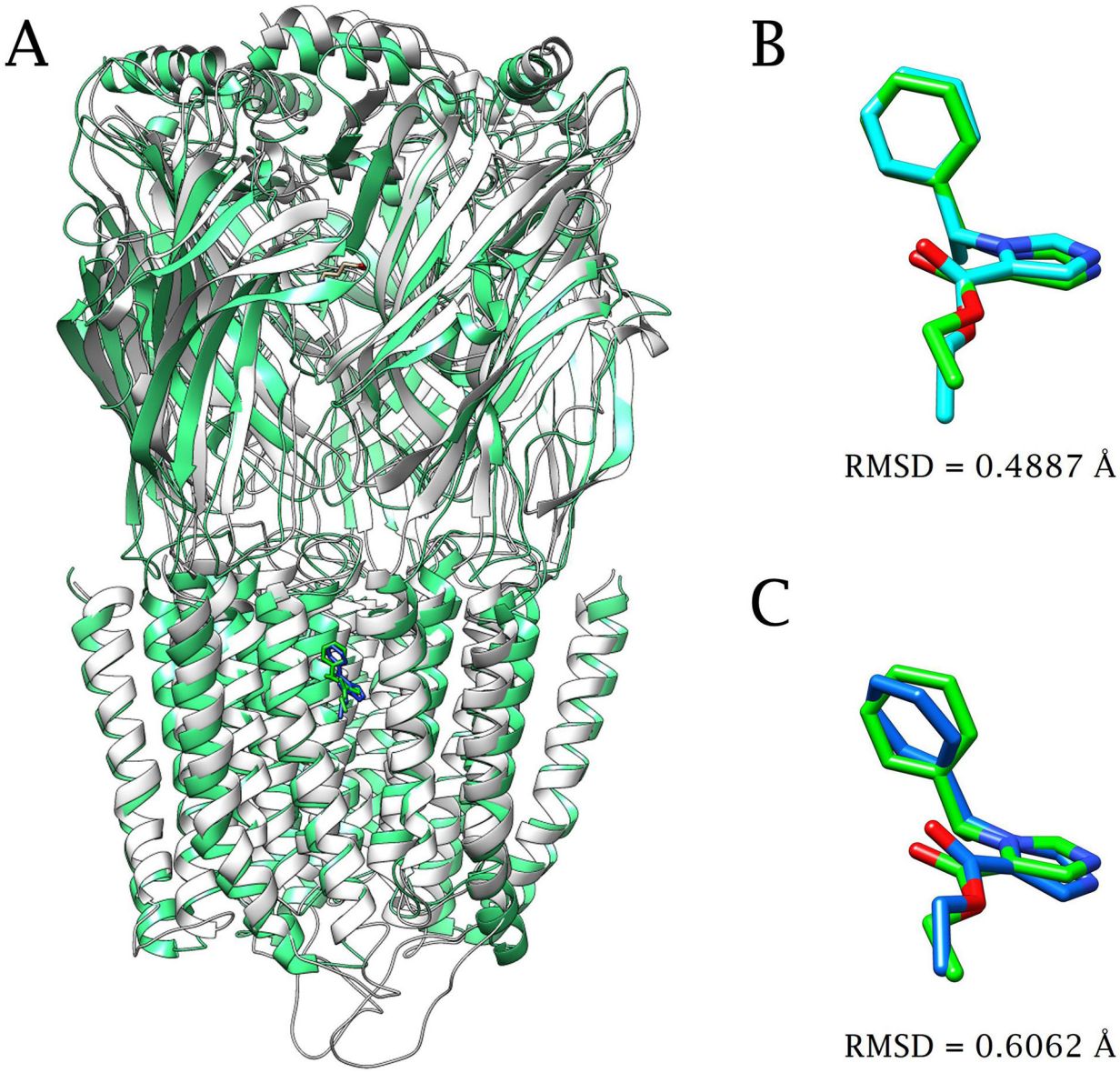

Figure 6.

Etomidate docking results in cryo-EM structure and homology-built model (HM) of α1β2γ2 $GABA_AR$. (A) Superposition of 6X3V (receptor and etomidate in green) and the adduct formed by etomidate (blue) docked within the HM built on 6HUJ (white). Ligand superposition and root mean squared deviation (RMSD) between the orientation of the cryo-EM R(+)-etomidate (green) and B. the docked conformer (cyano) within 6X3V, and C. the docking pose within the HM (blue). The docking poses obtained for R(+)-etomidate have an RMSD for the heavy atom of 0.489 Å (B) and 0.606 Å (C) from the original PDB coordinates and HM, respectively.

Author Manuscript Author Manuscript Author Manuscript Author Manuscript

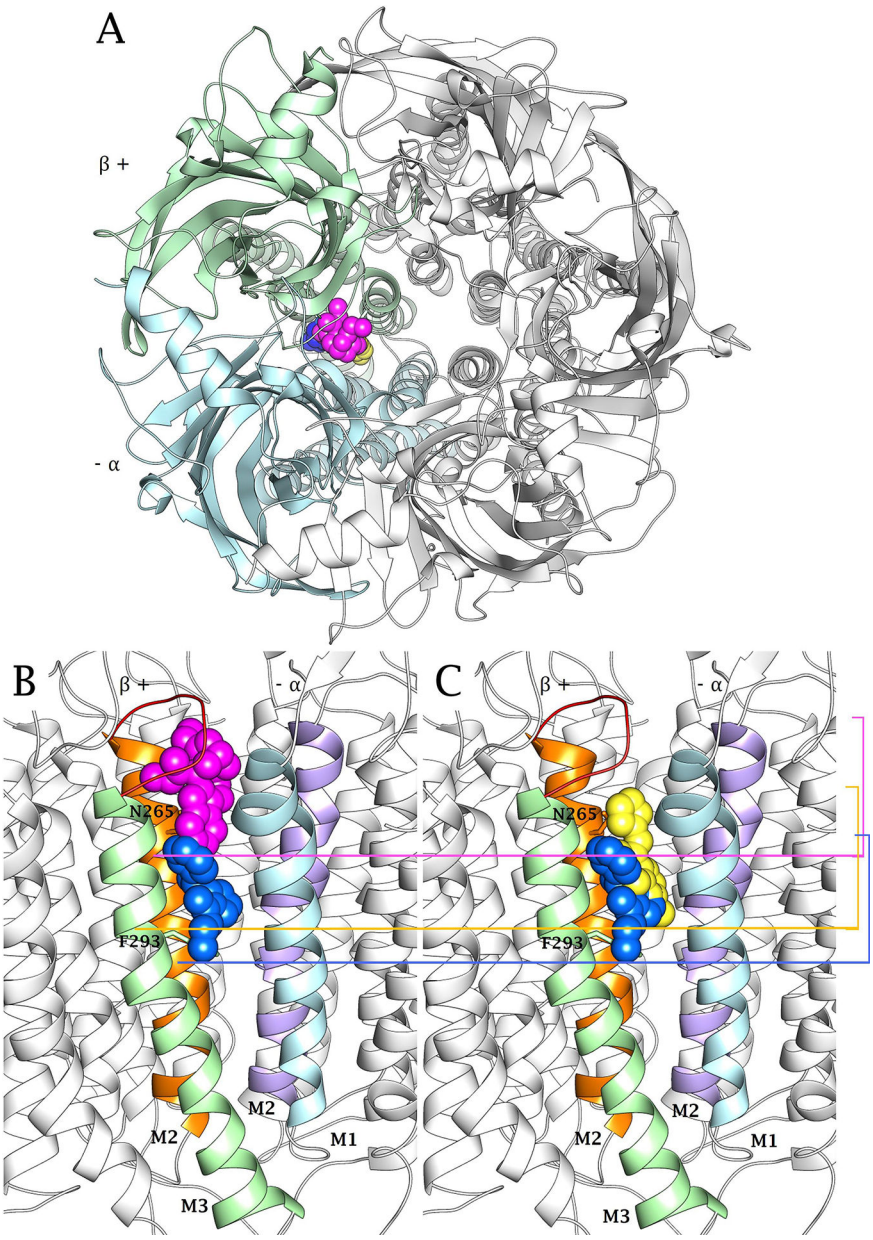

Figure 7.

Predicted binding mode of loreclezole, R(+)-etomidate, and (+)-catharanthine to the α1β2γ2 $GABA_AR$ model as an example of β2/3-containing receptors. (A) Transversal view of the $GABA_AR$ model showing the β2(+)(light blue)/α1(−)(light green) interface comprising the binding sites for loreclezole (yellow), R(+)-etomidate (blue), and (+)-catharanthine (purple) (represented as spheres). (B,C) Longitudinal view of the $GABA_AR$ model showing the binding area for each ligand (represented as spheres). The bottom limits, showed as colored lines and brackets, support non-overlapping areas for (+)-catharanthine (purple) and R(+)-etomidate (blue) (B) as well as partially overlapping areas for loreclezole (yellow) and R(+)-etomidate (blue) (C), and for loreclezole (yellow) and (+)-catharanthine (purple) [compare (B) and (C)], respectively. Interestingly, only (+)-catharanthine interacted with the

Author Manuscript Author Manuscript Author Manuscript Author Manuscript

ECD-TMD junction (red coil). Similitudes and differences with the dockings to the α2β1γ2 $GABA_AR$ model as an example of β1-containing receptors are included in Table 2.

Author Manuscript Author Manuscript Author Manuscript Author Manuscript

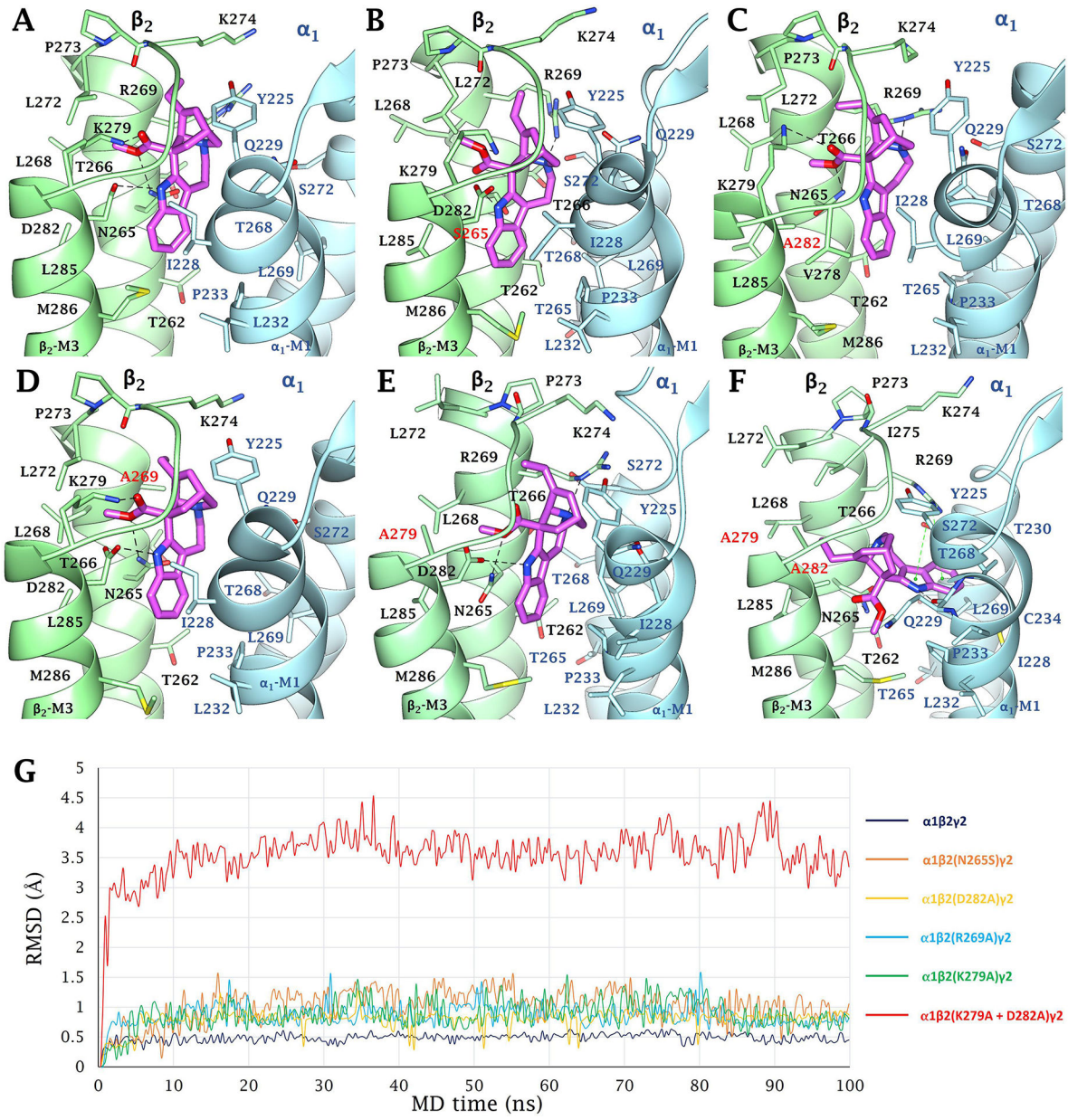

Figure 8.

Predicted binding mode of (+)-catharanthine at the wild-type and mutant $GABA_AR$ models. (+)-Catharanthine interacts with the β2(+)/α1(−) interface, establishing vdW contacts with several α1 (light blue) and β2 (light green) residues, and additional H-bond interactions delineated as follow: (A) (+)-Catharanthine (purple) forms H-bonds with β2-N265 and β2-R269 (both at TM2), β2-D282 (TM3), and K279 (TM2-TM3 loop), respectively (black dashed lines). In the α1β2(N265S)γ2 (B), α1β2(D282A)γ2 (C), α1β2(R269A)γ2 (D), α1β2(K279A)γ2 (E), and α1β2(D282A+K279A)γ2 (F) mutants, the respective H-bonds with S265, A282, A269, and A279 (highlighted in red) are lost, although vdW interactions with S265 and A269 are maintained. In the case of the β2(N265S) mutation, even considering that Ser can form a H-bond, it is shorter than Asp, consequently the

Author Manuscript Author Manuscript Author Manuscript Author Manuscript

distance and the binding geometry were not optimal for the formation of a H-bond with (+)-catharanthine. (G) RMSD plots for the molecular dynamics (MD) simulations (100 ns) of (+)-catharanthine docked to the different receptors. Similitudes and differences with the dockings to the α2β1γ2 $GABA_AR$ model as an example of β1-containing receptors are included in Table 2.

Author Manuscript Author Manuscript Author Manuscript Author Manuscript

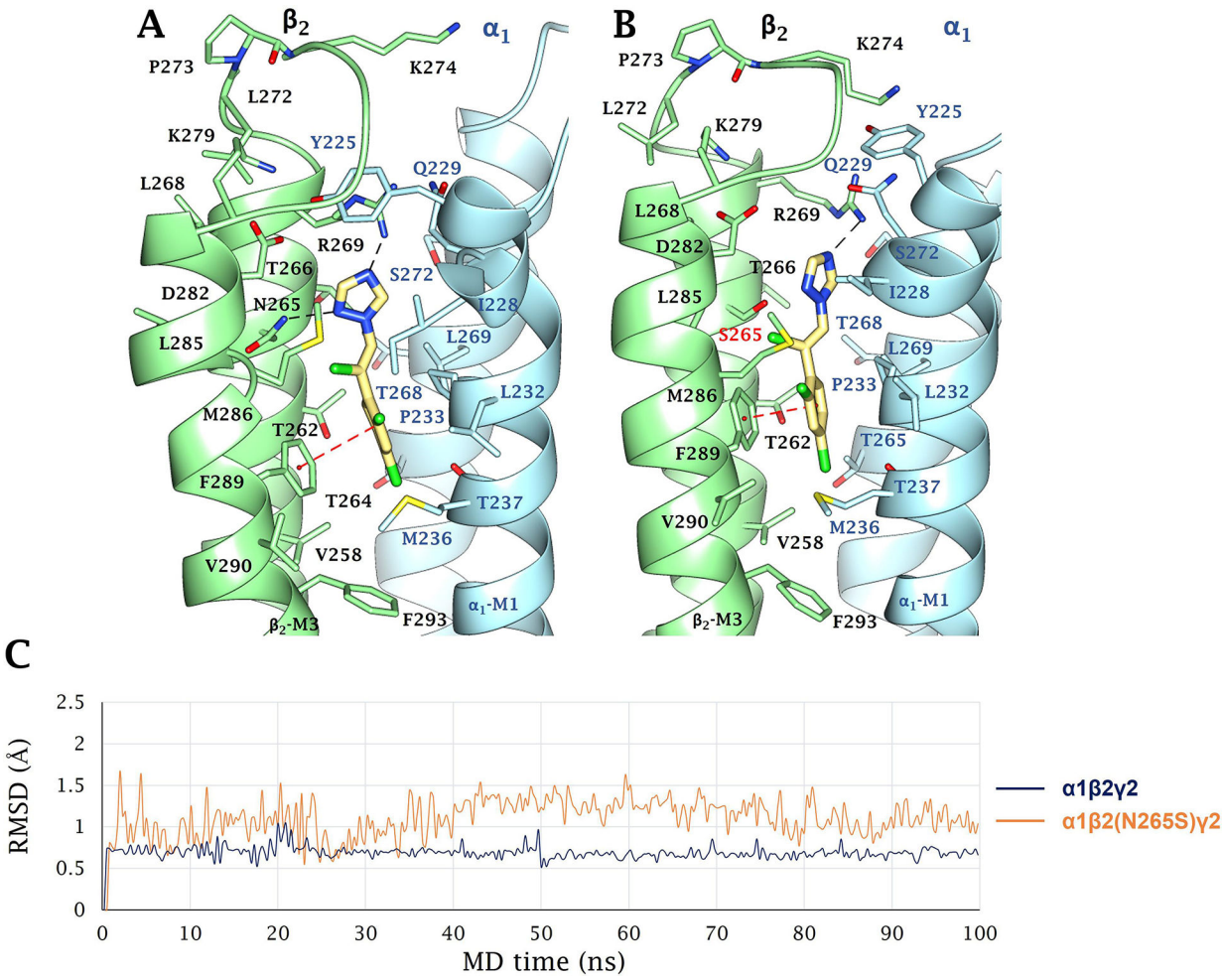

Figure 9.

Predicted binding mode of loreclezole at the wild-type and mutant $GABA_AR$ models. Loreclezole interacts with the β2(+)/α1(−) interface, establishing vdW contacts with several α1 (light blue) and β2 (light green) residues, and additional H-bond or π-π stacking interactions delineated as follow: (A) Loreclezole (yellow) forms H-bonds with β2-N265 and β2-R269 (black dashed lines), and a π-π stacking interaction with β2-F289 (TM3) (cyan dashed line). (B) In the α1β2(N265S)γ2 mutant, the respective H-bonds with β2-S265 (red) and β2-R269 lost stability over the MD course. (C) RMSD plots for the MD simulations (100 ns) of loreclezole docked to the different receptors. Similitudes and differences with the dockings to the α2β1γ2 $GABA_AR$ model as an example of β1-containing receptors are included in Table 2.

Author Manuscript Author Manuscript Author Manuscript Author Manuscript

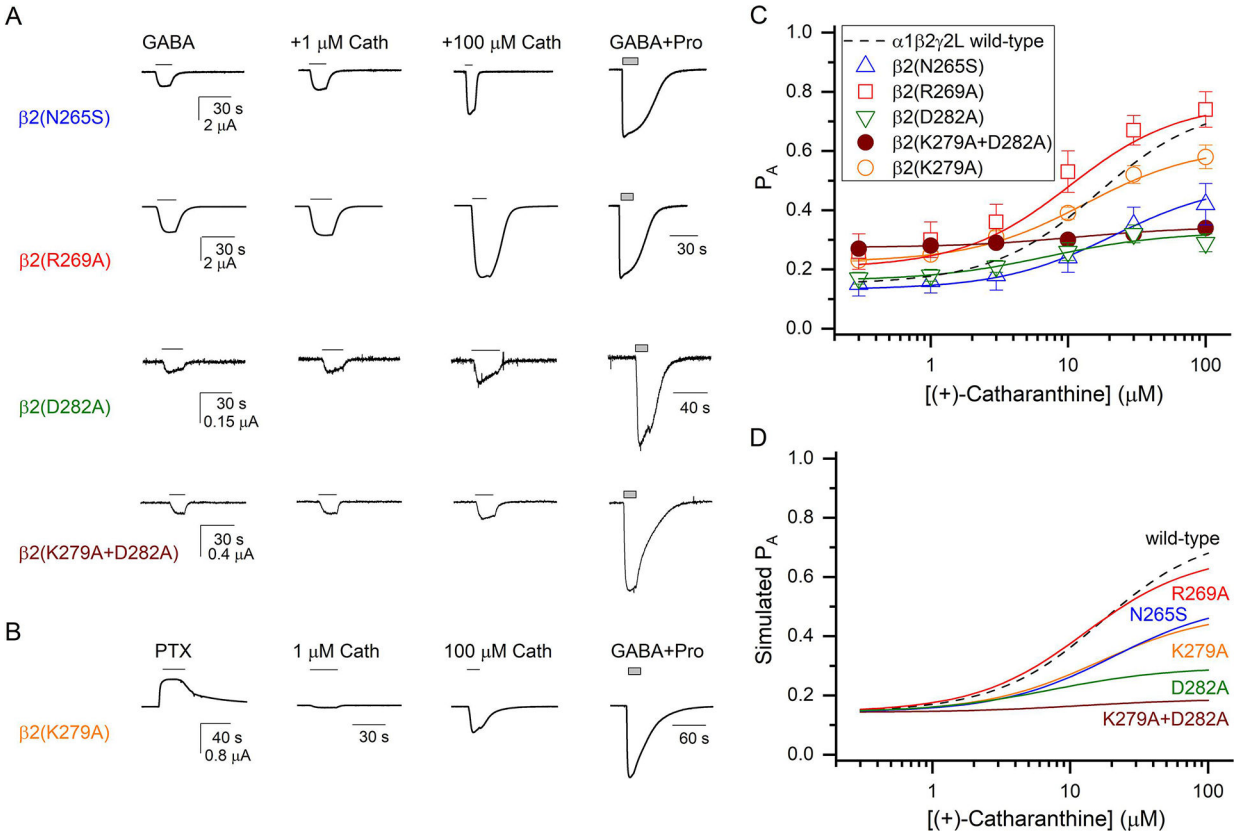

Figure 10.

(+)-Catharanthine-induced potentiation and activation of mutated α1β2γ2L $GABA_A$Rs. (A) Representative currents elicited by GABA (0.2–10 μM; P_A = 0.12–0.25) alone or in the presence of 1 or 100 μM (+)-catharanthine at α1β2γ2L $GABA_A$Rs containing the β2(N265S), β2(R269A), β2(D282A), or β2(K279A+D282A) mutation. For comparison, a trace showing the response to 1 mM GABA + 50 μM propofol (GABA+Pro) in the same cell is given for each mutant. (B) Representative currents elicited by 100 μM picrotoxin (PTX), 1 or 100 μM (+)-catharanthine, or 1 mM GABA + 50 μM propofol (GABA+Pro) at the α1β2(K279A)γ2L receptor. All currents were recorded at −60 mV. (C) Concentration-response relationships for (+)-catharanthine in the mutant receptors. The data points give mean ± SEM from 5 oocytes for each receptor. The curves show fits to (Eq. 1). The fitted K_{Cath} and c_{Cath} values are provided in Table 3. The curve for the wild-type α1β2γ2L $GABA_A$R (dashed line) is reproduced from Fig. 2. (D)Simulated concentration-response relationships for (+)-catharanthine in the wild-type and mutant receptors. The simulations were done using the fitted K_{Cath} and c_{Cath} values (Table 3) at a fixed background P_A of 0.15.

Author Manuscript

Author Manuscript

Author Manuscript

Author Manuscript

Table 1.

(+)-Catharanthine-elicited potentiation of wild-type and mutant $GABA_AR$s expressed in *Xenopus laevis* oocytes.

$GABA_AR$ Subtype	Data from Figure	(+)-Catharanthine maximal potentiation (%)[a]	(+)-Catharanthine relative potentiation (αxβ2/3γ2S)/(αxβ1γ2S)[b]
α1β1γ2S[a]	1B	269 ± 42 (4)	–
α1β2γ2S[a]	1B and 3B	739 ± 110 (11)	2.7
α1β3γ2S[a]	1B and 3A	646 ± 64 (10)	2.4
α2β1γ2S[a]	1B	211 ± 26 (5)	–
α2β3γ2S[a]	1B	691 ± 65 (5)	3.3
α2β3γ2S[a]	1B	728 ± 120 (4)	3.5
α1β1(M286C)γ2S[a]	3A	651± 120 (5)	–
α1β2(M286C)γ2S[a]	3B	264 ± 28 (6)	–

[a]Maximal potentiation of (+)-catharanthine determined at 100 μM [% over the control using EC_5 GABA (set at 100%) in the absence of (+)-catharanthine]. Data expressed as mean ± SEM.

[b]Comparative efficacy of (+)-catharanthine between β2/3- and its respective β1-containing $GABA_AR$ subtype (αxβ2/3γ2S)/(αxβ1γ2S)

Values in parentheses (n) correspond to the number of oocytes

Author Manuscript Author Manuscript Author Manuscript Author Manuscript

Table 2.

Residues involved in the docking of (+)-catharanthine and loreclezole to wild-type and mutant $GABA_AR$ models.

Ligand	$GABA_AR$ model	α1/2-Subunit Residues	β2/3-Subunit Residues
(+)-Catharanthine	α1β2/3γ2	Y225 (pre-TM1) I228 and Q229 (TM1)	**N265**, L268, and **R269** (TM2) L272, P273, K274, and **K279** (TM2-TM3 loop) **D282** and L285 (TM3)
	α2β1γ2	Y225 (pre-TM1) I228 and Q229 (TM1) S272 (TM2)	S265 *, L268, and **R269** (TM2) L272, P273, K274 and **K279** (TM2-TM3 loop) **D282** and L285 (TM3)
	α1β2(N265S)γ2	Y225 (pre-TM1) I228 and Q229 (TM1)	S265 *, L268, and **R269** (TM2) L272, P273, K274 and **K279** (TM2-TM3 loop) **D282** and L285 (TM3)
	α1β2(R269A)γ2	Y225 (pre-TM1) I228 and Q229 (TM1)	**N265**, L268, and A269 * (TM2) L272, P273, K274, and **K279** (TM2-TM3 loop) **D282** and L285 (TM3)
	α1β2(D282A)γ2	Y225 (pre-TM1) I228, Q229, and P233 (TM1)	**N265**, L268, and **R269** (TM2) L272, P273, K274, and **K279** (TM2-TM3 loop) A282 * and L285 (TM3)
	α1β2(K279A)γ2	Y225 (pre-TM1) I228, Q229, and P233 (TM1)	**N265**, L268, and **R269** (TM2) L272, P273, and K274 (TM2-TM3 loop) **D282** (TM3)
	α1β2(D282A+K279A)γ2	Y225 (pre-TM1) I228, **Q229**, T230 P233 and C234 (TM1) T268 and S272 (TM2)	**N265**, L268, T266, and R269 (TM2) A282 *, L285 and M286 (TM3)
Loreclezole	α1β2/3γ2	Q229, P233, and T237 (M1) T265 and L269 (M2)	V258, T262, **N265**, and **R269** (TM2) *F289* (TM3)
	α2β1γ2	Q229, P233, and T237 (TM1) T265 and L269 (TM2)	V258, T262, S265 *, and **R269** (TM2) *F289* (TM3)
	α1β2(N265S)γ2	Q229, P233, and T237 (TM1) T265 and L269 (TM2)	V258, T262, S265 *, and **R269** (TM2) *F289* (TM3)

Residues in **bold** form H-bonds. Residues in *italics* form π-π interactions. Underlined residues form π-cation interactions.

* Residues β2-S265, β2-A269, and β2-A282 form van der Waals interactions in the respective mutant.

Author Manuscript

Author Manuscript

Author Manuscript

Author Manuscript

Table 3.

Potentiation of the α1β2γ2 wild-type and mutant receptors by (+)-catharanthine.

Receptor	K_{Cath} (μM)[a]	c_{Cath}[b]	ΔG (kcal/mol)[c]	EC_{50} (μM)[d]	n_H[d]
α1β2γ2L	29.4±6.0	0.231±0.023	−1.76±0.12	13.5±1.8	1.66±0.33
α1β2(N265S)γ2L	23.9±2.5	0.390±0.021*	−1.12±0.07*	17.7±1.4	1.53±0.13
α1β2(R269A)γ2L	18.8±3.3	0.279±0.022	−1.53±0.11	9.3±1.2	1.29±0.10
α1β2(K279A)γ2L	17.8±1.6	0.421±0.034*	−1.04±0.10*	13.6±2.0	1.08±0.11
α1β2(D282A)γ2L	7.1±2.8*	0.630±0.039*	−0.55±0.07*	7.7±1.6	1.88±0.39
α1β2(K279A+D282A)γ2L	11.6±4.6[nd]	0.848±0.010[nd]	−0.19±0.01[nd]	15.8±5.9	1.30

[a] Estimated affinity of (+)-catharanthine for the resting receptor.

[b] Ratio of the affinities for the active and resting states. Higher efficacy is reflected in a lower c_{Cath} value.

[c] Values calculated from c_{Cath} as $N_{Cath}RT\ln(c_{Cath})$. The number of binding sites for (+)-catharanthine (N_{Cath}) was constrained to 2.

[d] Values estimated from curve-fitting to the Hill equation.

For wild-type and single mutant receptors, the concentration-response data from each oocyte were analyzed separately and are presented as mean ± SEM from 5 oocytes per receptor. For the β2(K279A+D282A) double mutant, the data from 5 oocytes were pooled and fitted using Eq. (1) or the Hill equation. The values give best-fit parameter ± standard error of the fit. Statistical comparison of K_{Cath}, c_{Cath}, and ΔG values in the mutants vs. wild-type was done using ANOVA with Dunnett's correction (StataIC 12, StataCorp LLC, College Station, TX).

*, $p < 0.01$; nd, not done.